THE CLEAVAGE OF IONIC MINERALS

THE CRYSTAL STRUCTURE OF BIXBYITE

AND THE C-MODIFICATION OF THE SESQUIOXIDES

Thesis

by

Maple D. Shappell

In partial fulfilment of the requirements
for the degree of Doctor of Philosophy

California Institute of Technology

Pasadena, California

1933

THE CLEAVAGE OF IONIC MINERALS

A B S T R A C T

Mineral cleavage can be resolved into two components; cleavability and optical effect. The electrical theory of matter in the solid state leads to a quantitative expression for the cleavability of ionic minerals

$$C_{\{hkl\}} = \frac{A_{(hkl)}}{\sum_i n_i s_i \cos \Theta_i}$$

Approximate values for s are obtainable by using the electrostatic bond strength. Systematic application to minerals whose constituent atoms have inert-gas cores gives good agreement with observation.

CONTENTS

1. INTRODUCTION

It has long been recognized that a close interrelationship must exist between the geometrical arrangement of the constituent particles of a mineral and the cleavage it exhibits; as a result the development of the theory of crystal structure has led to attempts to explain cleavage while at the same time work on cleavage has of necessity been required to gain an understanding of structure. Nevertheless in spite of its long standing the problem of cleavage has continued as one of great difficulty.

Cleavage has been defined[1] as "the natural fracture of a crystallized mineral yielding more or less smooth surfaces; it is due to minimum cohesion."

It is evident that the term cleavage should be resolved into two distinct parts, first a comparison of the work of separation, i.e. "cleavability", and second the nature of the surface fracture and its interaction with light. For example, the goniometric signal from the cleavage form {111} of diamond is strong - hence the cleavage is said to be perfect. The necessary distinction between these two phases of cleavage has not always been made. Cleavability is the more fundamental and the present investigation is largely restricted to a study of this property.

Experimentally cleavage is obtainable by several methods, of which the following are the more important.

1. Blow. This is likely to result in a general shattering of the material with the process largely one of shearing.
2. Wedge-action, e.g. with a knife. It can be either static or dynamic; in the former case pressure on the wedge is increased until fracture occurs while in the latter a number of blows on the wedge is made.

3. Bending. Analogous to the deflection of a beam.

4. Direct pull normal to the cleavage plane, i.e. the stress is a tension.

The second method is the one usually applied.[2] Up to the present time the experimental data on cleavage have been chiefly of a qualitative nature.

2. Previous Work on Cleavage

Cleavage investigations have taken in general two distinct directions; either that cleavage can be accounted for by the point geometry of the crystal or that it depends on the breaking of bonds between the atoms.

The first method is a development of the fundamental researches of Bravais.[3] He held that cleavage is obtained parallel to the plane of greatest net density and that in case cleavage is obtained parallel to several forms the ease of obtaining it decreases in the order of the decreasing net densities. However since the net densities are inversely proportional to the lattice face areas, he used the latter for calculating relative values. Moreover since net density and interplanar distance are proportional, he gave as an alternative condition for most complete cleavage that the interplanar distance be greatest.

Sohncke[4] used the interplanar distance condition but because of lattice interpenetration added to it the further condition that the cleavage planes be parallel to planes where the tangential cohesion is greatest. This is because interpenetration often causes in a sequence of parallel planes several of them to be grouped closer together

into a layer which is repeated at regular intervals. The assumption being made that such layers are more strongly held together the result is greater tangential cohesion. When Bravais' theory was systematically applied to crystals of the trigonal and hexagonal system, Tertsch[5] found numerous exceptions. The application of Sohncke's condition requires knowledge of the crystal structure. Basing their conclusions on x-ray determinations, Ewald and Friedrich[6] independently came to the same condition as Sohncke. Stark[7] considering crystals in which the atoms can be considered to exist as ions, related cleavage to the repulsion of like ions of adjacent net planes approaching each other during a shearing process; however the possible cleavage faces are too numerous for this to be unique condition. Scharizer[8] postulated that the adjoining planes of two layers must be similar, the same holding true for a non-layer sequence; this condition evidently permits the application of Stark's relation. Niggli[9], by summing the number of electrons of the atoms at the lattice points, converted Bravais' net density into planes of electron density. Beckenkamp's[10] treatment is essentially a combination of the conditions of Sohncke and Stark. Parker[11] has applied Niggli's method to the structure of octahedrite.

The concept of conditioning cleavage on the breaking of bonds between particles was used by Barlow[12] as a result of his studies on the close-packing of spherical particles; the bonds broken in the process are not necessarily those which under static conditions have least strength. He gave as a probable condition that cleavage planes separate opposed unlike particles, a condition directly opposite to that of Stark. Ewald[13] postulated that cleavage will take place where the fewest bonds are broken. Relative calculated values per unit area

for diamond gave agreement with observation; however discrepancies arising in a later study[14] caused this postulate to be questioned and the condition of the previous paragraph to be set up as essential. Huggins[15] came to the conclusion that new crystal surfaces should be left electrically neutral, that weak bonds would be ruptured in preference to strong bonds but that where all bonds are equally strong, the cleavage plane would break fewest bonds per unit area. He considered that the inclination of the bond to the cleavage normal could be neglected. Tertsch,[16,18] considering the problem as one of attractive and repulsive forces between ions, calculated a value for the force across various possible cleavage planes, the minimum indicating the most cleavable. The inclination of the individual force directions to the cleavage normal is taken into account by using its direction cosine. Pauling[17] calculated the density (bonds per unit area) of Al-O-Si bonds for cleavage in several aluminosilicates; he found that ease of cleavage decreases as bond-density increases.

3. Derivation of a Quantitative Expression for Cleavability.

Cleavage in minerals is one phase of the phenomenon of the cohesion of matter in the solid state; it accordingly is concerned with the interactions of the constituent particles when disturbed by mechanical forces from the configuration taken by them at equilibrium. The necessary and sufficient condition for equilibrium in a conservative system is that[19]

$$(\delta S)_E = 0,$$

where S is the entropy and E the energy. A more workable criterion is gained however by using the free energy, F, which is a function of S. The condition then becomes in the commonly used notation of Lewis and Randall[20]

$$dF = 0. \qquad (1)$$

In the wave equation of quantum mechanics,[21]

$$\nabla^2 \psi + \frac{8\pi^2 \mu}{h^2} (W - V) \psi = 0,$$

the product of the eigenfunction ψ by its complex conjugate $\bar{\psi}$ may be interpreted as the electron density ρ, i.e. the probability of the configuration of the system. The distribution of ρ has been shown to be spherically symmetrical about the nucleus for atoms and ions having completed subgroups of electrons.[22,23] It follows that the n electrons in an ion can be considered in effect as if located at the center of symmetry.[24] Under the assumption that polarization can be neglected, the center of symmetry for both the resultant positive and negative charges coincide, permitting a system of ions to be treated mathematically as discrete point charges (plus a repulsive term to

be taken into account later) of value

$$\pm z = Z - n, \qquad (2)$$

where z denotes the valence, Z the charge on the nucleus and n the number of electrons. Since the atoms are in thermal agitation about a mean position it is unnecessary to refer the system to a temperature of absolute zero and accordingly the lattice constants as determined at ordinary temperatures can be used.

In the equilibrium condition the quantity F is given by

$$F = E + P V - T S,$$

where E is the total energy, P the pressure, V the volume, T the absolute temperature and S the entropy of the system. The term containing the entropy drops out at the absolute zero, and if the region surrounding the system is void of matter the $P V$ term also disappears. Hence under these conditions

$$F = E. \qquad (3)$$

It is convenient to consider the crystal as at absolute zero with a volume energy content E obtained by using the ordinary lattice constants without extrapolating to zero, since the difference of energy is small.[25] ~~(Around 1% or about 2 large calories per mole for crystals of the halite type).~~

A method of evaluating E for ionic crystals is known,[26, 27] the energy expressed in either ergs or calories per mole, being designated as the lattice energy. The results of crystal structure determinations while giving the configuration of ions in a crystal say nothing as to the interactions between them.[28] It is known from Earnshaws Theorem[29] that in classical electrostatics a system of electric charges alone cannot be in equilibrium; a repulsive term is accordingly required.

The potential law between two ions is assumed as a first approximation to be

$$\phi = -\frac{z_1 z_2 e^2}{r} + \frac{b}{r^n} \qquad (4)$$

where z_1 and z_2 are the charges on the ions obtained from Equation 2, e the electron charge, r the distance between ions, b a proportionality constant and n the repulsive exponent, which ordinarily can be taken as approximately equal to nine. The equilibrium energy of a unit cell is given by

$$\Phi = -\frac{z_1 z_2 e^2 A}{r_o}\left(1 - \frac{1}{n}\right) \qquad (5)$$

where b has been eliminated, r_o is the equilibrium distance between adjacent ions, and A is the Madelung constant. The energy due to the repulsive term is evidently small. Dividing Φ by p, the number of molecules in the unit cell, and multiplying by N, Avogadro's number, gives

$$E = \frac{N}{p}\Phi. \qquad (6)$$

Accordingly if a system of ions, e.g. a crystallized mineral, satisfies the condition

$$dE = 0 \qquad (7)$$

the system is in equilibrium and its energy is given by Equation 6.

When cleavage takes place the crystal is separated along a surface into two parts, each containing a volume energy, E_1 and E_2, and in addition if A is the area of the cleavage plane the area of surface has been increased by $2A$. On separation the interaction energy E_{12} will equal zero since the ions have only a small radius of influence; there enters[30,31,32,33] however a surface free energy, $2\sigma A$,

whose absolute specific value is given by

$$\sigma = \frac{E_{12}}{2A}. \tag{8}$$

The value of E_{12} can be obtained by a method of a similar nature to that used in calculating E. The change in free energy then becomes

$$F = F_1 - F_2 = E_{12} = 2\sigma A. \tag{9}$$

For a sequence of variously oriented planes through a crystal, a series of values is obtained for ΔF and the plane of easiest separation is given by

$$\Delta F = \text{minimum}. \tag{10}$$

Accordingly the cleavability C of a mineral is defined as the reciprocal of the change in free energy

$$C = \frac{1}{\Delta F}. \tag{11}$$

In terms of unit area Equation 11 becomes

$$C_{\{hkl\}} = \frac{1}{2\sigma}. \tag{12}$$

If the volume remains constant which is approximately correct[34] Equation 10 becomes for the cleavage form the surface energy law of Gibbs[35] and Curie[36,37]

$$\Sigma \sigma s = \text{minimum} \tag{13}$$

where s is the face area. It may be mentioned that a fictitious "surface tension" is often conveniently used in the mathematical calculations instead of surface energy since the dimensions are the same for both.[38,39,40] A 3-dimensional method to exhibit the value of for various orientations of the separation surface in a crystal is known.[41,42,43,44,45] If normals to the plane are drawn from a center of coordinates within the crystal[46] proportional to σ, their extremities form a surface in which the minima are depressions. These

will be symmetrically placed according to the symmetry of the crystal and may consist of secondary as well as primary minima, the secondary being due to a lesser degree of cleavability.

The calculation of the surface energy σ needed for Equation 12 is involved and has only been carried out for the most simple ionic configurations; moreover it is desirable to express the cleavability in terms more closely related to the mechanical properties of the crystal rather than in terms of energy. This can be done by identifying $E_{1,2}$ of Equation 8 with the mechanical work W done on the system.[47,48,49,50,51] Equation 12 then becomes

$$C_{\{hkl\}} = \frac{A_{(hkl)}}{W} . \qquad (14)$$

Since the maximum force per unit area is the tensile strength, i.e. the breaking strength of the crystal for the direction of the normal to the cleavage plane, $W = k S$ where k is a parameter which without loss of generality can be placed equal to unity. Cleavability is the reciprocal of the tensile strength,

$$C_{\{hkl\}} = \frac{1}{S_{(hkl)}} . \qquad (15)$$

The force between pairs of ions having the cleavage surface interposed between them can be considered as in the nature of a bond. On stressing the crystal until S is reached each of these bonds will have a value s giving as its normal component $s \cos \Theta$. (see fig. 1) Let the number of such bonds for each i^{th} ion be denoted by n, then the maximum force normal to the face area is given by

$$F_M = \sum_i n_i s_i \cos \Theta_i .$$

Since $S_{(hkl)} = F_M / A_{(hkl)}$, Equation 15 now becomes

$$C_{\{hkl\}} = \frac{A_{(hkl)}}{\sum_i n_i s_i \cos \Theta_i} . \qquad (16)$$

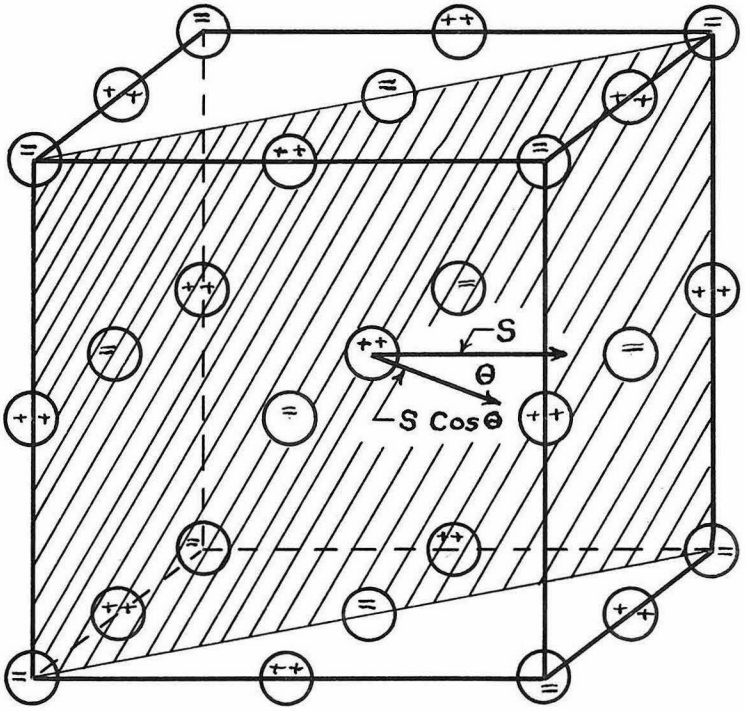

Fig. 1. The (110) plane for periclase showing the relationship of s and θ to the cleavage normal.

A simple estimate of the bond strength s is obtainable from the coordination theory of ionic structures.[52] It is evident from crystal geometry that the strongest bonds are those between cations and anions of the coordinated polyhedra, Hence the electrostatic valence bond strength equal to the charge on the cation z divided by the coordination number V,

$$S = \frac{z}{V}$$

can be used as a first approximation.[53] The angular change in θ from its equilibrium value is usually small and in general may be neglected. The expression for cleavability, Equation 16, may now be applied to ionic minerals.

4. Selection of Ionic Minerals.

Minerals are a heterogeneous group of substances and a classification is accordingly necessary in order to have some basis of selection for those likely to be amenable to a simple treatment.

A rational basis for grouping is to be found in an examination of the structure of the elements. If the valence electrons are stripped from the atoms of the periodic table, the elements can be divided into two main groups, (1) Ionic, (2) Covalent.

The covalent group is composed largely of elements whose cores have an outer shell of eighteen electrons. The bond between such elements is predominately due to the sharing of electrons, requiring treatment by quantum mechanical methods. Moreover due to their ease of deformation, polarization effects further complicate the cohesive phenomena of minerals composed of such atoms. The elements of this group are those with atomic numbers 26 (Fe) to 35 (Br), 44 (Ru) to 53 (K), and 76 (Os) to 84 (Po). Minerals consisting essentially of atoms from this group will be eliminated from this investigation.

The ionic group have cores whose electron configuration is that of the inert gases, hence with an outer shell of eight electrons. As previously shown the bonds between such ions in the solid state can be considered as of an electrostatical nature. The superimposed effects of a dipole field can be greatly reduced by restricting the anions to those of the smallest atomic radii, namely oxygen $O^{=}$ and fluorine F^{-}. The hydroxyl ion OH^{-}, where it is a subordinate constituent as in the amphiboles, will be assumed to give no appreciable polarization effect.

The fundamental nature of this two-fold grouping has been shown by several recent geochemical investigations.[54,55,56]

As a basis for systematic application of the cleavability expression, ionic minerals treated in this study are classified as follows:

A. Simple ions

I. Binary system, A - X.

Class 1. A : x = 1.

Villiaumite, NaF. (Halite structure)
Bromellite, BeO. (Wurtzite structure)
Periclase, MgO. (Halite structure)
Lime, CaO. (Halite structure)

Class 2. A : x = 2 : 3.

Corumdum, Al_2O_3.

Class 3. A : x = 1 : 2.

Sellaite, MgF_2. (Rutile structure)
Fluorite, CaF_2.
Quartz, SiO_2.
Cristobalite, SiO_2.
Tridymite, SiO_2.
Rutile, TiO_2.
Octahedrite, TiO_2.
Brookite, TiO_2.

II. Ternary system, A - B - X.

Spinel, $MgAl_2O_4$.

B. Complex radical, ARX_3.

Calcite, $CaCO_3$.

C. Silicates.[57,58]

I. Independent tetrahedral groups.

Class 1. Single SiO_4 groups.

Phenacite, Be_2SiO_4.
Kyanite, Al_2OSiO_4.
Topaz, $Al_2SiO_4F_2$.
Zircon, $ZrSiO_4$.
Grossularite (garnet group), $Ca_3Al_2(SiO_4)_3$.

C. Silicates (cont)

Class 2. Si_2O_7 groups.

Melilite, $Ca_2MgSi_2O_7$.

II. Tetrahedral chains.

Class 1. Single chains.

Diopside (pyroxene group), $CaMgSi_2O_6$.

Class 2. Double chains

Tremolite (amphibole group), $Ca_2Mg_5(Si_4O_{11})_2(OH)_2$.

III. Tetrahedral planes.

Muscovite, $KAl_2(Si_3Al)O_{10}(OH,F)_2$.

IV. Three-dimensional network of tetrahedra.

Sodalite, $Na_4Al_3Si_3O_{12}Cl$.

5. Structure and Cleavage.

For most of the structural arrangements given below reference is made to Ewald, P.P. and Hermann, C., "Strukturbericht, 1913-1928," Z.Krist. Ergänzungsband (1931). In the comparison of calculated relative values with observation the work of Dana (see Ref. 1) is used. It is found that electrical neutrality of cleavage surfaces where it does not follow as a result of a plane of cleavage is obtainable by a non-planar cleavage surface; possible cleavage surfaces are considered to be electrically neutral. In cases where a cleavage form has several alternative cleavage surfaces the most probable is taken to be the one giving the highest value for the cleavability. Cleavability values marked by a star denote cases where it is probable that the angular change in Θ cannot be neglected.

Villiaumite, Periclase and Lime.

Structural characteristics: Cubic, Γ_c' , O_h^5 . Z = 4. Villiaumite, NaF, a = 4.62 Å; periclase, MgO, a = 4.20 Å; lime, CaO, a = 4.80 Å.

Coordination: octahedra of anions.

Areas: Villiaumite, $A_{(100)} = 21.15$ Å^2, $A_{(110)} = 33.65$ Å, $A_{(111)} = 36.65$ Å^2
Periclase, $A_{(100)} = 17.63$ Å^2, $A_{(110)} = 24.93$ Å^2, $A_{(111)} = 30.54$ Å^2
Lime, $A_{(100)} = 23.00$ Å^2, $A_{(110)} = 32.52$ Å^2, $A_{(111)} = 39.84$ Å^2

Bond strengths: Villiaumite, $s_{Na-F} = 1/6$. Periclase, $s_{Mg-O} = 1/3$.
Lime, $s_{Ca-O} = 1/3$.

Summations: Villiaumite, $\Sigma\,(100) = 4 \times 1/6 \times 1.00(\Theta = 0°) = 0.67$, $\Sigma(110) = 8 \times 1/6 \times 0.71(\Theta = 45°) = 0.95$, $\Sigma\,(111) = 12 \times 1/6 \times 0.82(\Theta = 35°) = 1.64$.
Periclase, $\Sigma\,(100) = 4 \times 1/3 \times 1.00(\Theta = 0°) = 1.33$, $\Sigma\,(110) = 8 \times 1/3 \times 0.71(\Theta = 45°) = 1.89$, $\Sigma\,(111) = 12 \times 1/3 \times 0.82(\Theta = 35°) = 3.28$.
Lime, same as periclase.

TABLE 1. Cleavabilities of Villiaumite, Periclase and Lime.

Form		{100}	{110}	{111}
Type		closed cubic	closed dodecahedral	closed octahedral
Number of faces		6	12	8
		Villiaumite		
Cleavability	Calc.	31.5	31.5*	22.3
	Obs.[59]	complete	-	-
		Periclase		
Cleavability	Calc.	13.2	13.2*	9.3
	Obs.	Perfect	-	Less distinct
		Lime		
Cleavability	Calc.	17.2	17.2*	12.1
	Obs.[60]	Complete	Possibly	-

Remarks: The separation surfaces for {100} are coplanar ions.

Bromellite

Structural characteristics: Hexagonal, Γ_h , C_{6v}^4, Z = 4.

Lattice constants: a = 2.69 Å, C = 4.37 Å.

Composition: BeO. Coordination: Be-O tetrahedra.

Areas: $A_{(0001)} = 6.24$ Å^2, $A_{(10\bar{1}0)} = 11.75$ Å^2, $A_{(10\bar{1}1)} = 13.4$ Å^2, $A_{(11\bar{2}0)} = 20.35$ Å^2.

Bond strengths: $s_{Be-O} = 1/2$.

Summations: $\Sigma\,(10\bar{1}0) = 2 \times 1/2 \times 0.94(\Theta = 20°) = 0.94$, $\Sigma\,(0001) = 1 \times 1/2 \times 1.00(\Theta = 0°) = 0.50$, $\Sigma\,(11\bar{2}0) = 4 \times 1/2 \times 0.87(\Theta = 30°) = 1.74$, $\Sigma\,(10\bar{1}1) = 1 \times 1/2 \times 1.00(\Theta = 0°) + 2 \times 1.2 \times 0.71(\Theta = 45°) = 1.21$

TABLE 2. Cleavability of Bromellite.

Form	$\{10\bar{1}0\}$	$\{0001\}$	$\{11\bar{2}0\}$	$\{10\bar{1}1\}$
Type	open prismatic	open basal	open prismatic	closed bipyramidal
Number of faces	6	2	6	12
Cleavability Calc.	12.5	12.5*	11.7	11.1
Obs.	Distinct	Doubtful	-	-

Remark: According to Groth (see Ref. 6D) there is no distinct cleavage.

Corundum

Structure characteristics: Trigonal, Γ_{rh}, D_{3d}^{6}. Z = 2.

Lattice constants: a = 5.12 Å, α = 55°17'.

Composition: Al_2O_3. Coordination: Al-O octahedra.

Areas: $A_{(100)} = 18.16$ Å^2, $A_{(111)} = 19.20$ Å^2, $A_{(110)} = 49.28$ Å^2, $A_{(2\bar{1}\bar{1})} = 60.57$ Å, $A_{(10\bar{1})} = 104.79$ Å^2.

Bond strength: $s_{Al-O} = 1/2$.

Summations: Σ (110) = 8 x 1/2 x 0.98(θ = 10°) = 3.92,

$\Sigma(\bar{2}\bar{1}1) = 8 \times 1/2 \times 0.77(\Theta = 40°) + 8 \times 1/2 \times 0.71(\theta = 45°) = 5.92$,

$\Sigma(111) = 3 \times 1/2 \times 0.71(\Theta = 45°) + 3 \times 1/2 \times 0.64(\Theta = 50°) = 2.02$,

$\Sigma(10\bar{1}) = 6 \times 1/2 \times 0.77(\theta = 40°) + 6 \times 1/2 \times 0.71(\Theta = 45°) +$

$12 \times 1/2 \times 0.64(\Theta = 50°) + 12 \times 1/2 \times 0.50(\Theta = 60°) = 11.28$,

$\Sigma(100) = 2 \times 1/2 \times 0.42(\Theta = 65°) + 2 \times 1/2 \times 0.71(\Theta = 45°) +$

$2 \times 1/2 \times 0.98(\Theta = 10°) = 2.11$.

TABLE 3. Cleavability of Corundum

Form	x-ray unit	{110}	{2$\bar{1}\bar{1}$}	{111}	{10$\bar{1}$}	{100}
	Dana	{10$\bar{1}$1}	{10$\bar{1}$0}	{0001}	{11$\bar{2}$0}	{02$\bar{2}$1}
Type		closed rhombohedral	Open prismatic	Open basal	Open prismatic	Closed rhombohedral
Number of faces		6	6	2	6	6
Cleavability	Calc.	12.4	10.2	9.5	9.2	8.6
	Obs.	-	-	-	-	-

Remarks: Parting on {110} often prominent.

Fluorite

Structure characteristics: Cubic, Γ_c', O_h^5. Z = 4.

Lattice constant: a = 5.45 Å. Composition: CaF_2.

Coordination: Ca-F hexahedra.

Areas: $A_{(100)} = 29.7$ Å^2, $A_{(110)} = 42.0$ Å^2, $A_{(111)} = 51.4$ Å^2.

Bond strength: $s_{Ca-F} = 1/4$.

Summations: Σ (110) = 8 x 1/4 x 0.71(Θ=45°) = 1.42,

Σ (111) = 8 x 1/4 x 1.00(Θ =0°) = 2.00, Σ (100) = 8 x 1/4 x 0.577 (Θ =54°) = 1.15

TABLE 4. Cleavability of Fluorite.

Form		{110}	{111}	{100}
Type		closed dodecahedral	closed octahedral	closed cubic
Number of faces		12	8	6
Cleavability	Calc.	29.7*	25.7	25.7*
	Obs.	occasionally distinct[62]	perfect	-

Quartz

Structure characteristics: Hexagonal, Γ_h, D_6^5 or D_6^4. Z = 3.

Lattice constants: a = 5.01 Å, c = 5.47 Å. Composition: SiO_2.

Coordination: Si-O tetrahedra. High temperature modification.

Areas: $A_{(0001)} = 21.8$ Å^2, $A_{(10\bar{1}0)} = 27.40$ Å^2, $A_{(10\bar{1}1)} = 35.00$ Å, $A_{(11\bar{2}0)} = 47.6$ Å^2.

Bond strength: $s_{Si-O} = 1$.

Summations: $\Sigma(10\bar{1}1) = 1 \times 1 \times 0.87(\Theta = 30°) + 1 \times 1 \times 1.00(\Theta = 0°) = 1.87$,

$\Sigma(11\bar{2}0) = 2 \times 1 \times 0.50(\Theta = 60°) + 2 \times 1 \times 0.87(\Theta = 30°) = 2.74$,

$\Sigma(0001) = 2 \times 1 \times 0.64(\Theta = 50°) = 1.28$, $\Sigma(10\bar{1}0) = 1 \times 1 \times 0.87$ $(\Theta = 30°) + 1 \times 1 \times 0.82(\Theta = 35°) = 1.69$.

TABLE 5. Cleavability of Quartz.

Form		$\{10\bar{1}1\}$	$\{11\bar{2}0\}$	$\{0001\}$	$\{10\bar{1}0\}$
Type		closed bipyramidal	open prismatic	open basal	open prismatic
Number of faces		12	6	2	6
Cleavability	Calc.	18.7	17.4	17.0	16.2
	Obs.	difficult and seldom observed	more difficult	more difficult	-

Remark: According to Rogers[63] imperfect $\{10\bar{1}1\}$ cleavage is rather common, especially in thin section.

Christobalite

Structure characteristics: Cubic, Γ_c^1, O_h^7, Z = 8.

Lattice constant: a = 7.12 Å. Composition: SiO_2.

Coordination: Si-O tetrahedral framework. High temperature modification.

Areas: $A_{(100)} = 50.69$ Å^2, $A_{(110)} = 71.7$ Å^2, $A_{(111)} = 87.85$ Å^2.

Bond strength: $s_{Si-O} = 1$.

Summations: $\Sigma\,(100) = 4 \times 1 \times 0.57(\Theta = 55°) = 2.28$,

$\Sigma\,(110) = 4 \times 1 \times 0.82(\Theta = 35°)$, $\Sigma\,(111) = 4 \times 1 \times 1.00$ $(\Theta = 0°) = 4.00$

$= 3.28$

TABLE 6. Cleavability of Christobalite.

Form		{100}	{111}	{110}
Type		closed cubic	closed octahedral	closed dodecahedral
Number of faces		6	8	12
Cleavability	Calc.	22.2	22.0	21.9
	Obs.	-	-	-

Tridymite

Structure characteristics: Hexagonal, Γ_h, D^4_{6h}. Z = 4.

Lattice constants: a = 5.03 Å, c = 8.22 Å. Composition: SiO_2.

Coordination: Framework of Si-O tetrahedra. High temperature modification.

Areas: $A_{(0001)} = 21.91$ Å^2, $A_{(10\bar{1}0)} = 41.35$ Å^2, $A_{(10\bar{1}1)} = 46.5$ Å^2. $A_{(11\bar{2}0)} = 71.62$ Å^2.

Bond strength: $s_{Si-O} = 1$.

Summations: $\Sigma\ (10\bar{1}0) = 2 \times 1 \times 0.94(\theta = 20°) = 1.88$, $\Sigma\ (0001) = 1 \times 1 \times 1.00(\theta = 0°) = 1.00$, $\Sigma\ (11\bar{2}0) = 4 \times 1 \times 0.87(\theta = 30°) = 3.48$, $\Sigma\ (10\bar{1}1) = 1 + 1 \times 1.00(\theta = 0°) + 2 \times 1 \times 0.64(\theta = 50°) = 2.28$.

TABLE 7. Cleavability of Tridymite.

Form		$\{10\bar{1}0\}$	$\{0001\}$	$\{11\bar{2}0\}$	$\{10\bar{1}1\}$
Type		open prismatic	open basal	open prismatic	closed bipyramidal
Number of faces		6	2	6	12
Cleavability	Calc.	22.0	21.9	20.6	20.4
	Obs.	not distinct	-	-	-

Remark: Parting sometimes observed $\parallel \{0001\}$

Sellaite and Rutile

Structure characteristics: Tetragonal, Γ_t , D_{4h}^{14}. Z = 2.

Lattice constants: Sellaite, MgF_2, a = 4.64 Å, c = 3.06 Å;

Rutile, TiO_2, a = 4.58 Å, c = 2.95 Å.

Areas: Sellaite, $A_{(100)}$ = 14.2 Å, $A_{(110)}$ = 20.1 Å, $A_{(001)}$ = 21.53 Å, $A_{(111)}$ = 29.41 Å. Rutile, $A_{(100)}$ = 13.51 Å, $A_{(110)}$ = 19.18 Å, $A_{(001)}$ = 20.94 Å, $A_{(111)}$ = 28.40 Å.

Bond strengths: $s_{Mg-F} = 1/3$, $s_{Ti-O} = 2/3$.

Summations: Sellaite (1/2 those of rutile), Σ (100) = 0.47, Σ (110) = 0.67, Σ (001) = 0.94, Σ (111) = 1.76. Rutile, Σ (100) = 2 x 2/3 x 0.71(Θ =45°) = 0.94, Σ (110) = 2 x 2/3 x 1.00(Θ =0°) = 1.33, Σ (001) = 4 x 2/3 x 0.71(Θ = 45°) = 1.88, Σ (111) = 2 x 2/3 x 1.00(Θ =0°) + 2 x 2/3 x 0.64(Θ =50°) + 4 x 2/3 x 0.50(Θ =60°) = 3.52.

TABLE 8. Cleavability of Sellaite and Rutile.

Form		{100}	{110}	{001}	{111}
Type		open prismatic	open prismatic	open basal	closed bipyramidal
Number of faces		4	4	2	8
Sellaite					
Cleavability	Calc.	30.1	30.1	23.2	16.7
	Obs.	perfect	perfect	-	-
Rutile					
Cleavability	Calc.	14.4	14.4	11.1	8.1
	Obs.	distinct	distinct	-	traces

Octahedrite

Structure characteristics: Tetragonal, Γ_t', D_{4h}^{19}. Z = 4.

Lattice constants: a = 3.73 Å, c = 9.37 Å. Composition: TiO_2

Coordination: Ti-O octahedra.

Areas: $A_{(001)} = 13.94$ Å^2, $A_{(100)} = 34.93$ Å^2, $A_{(101)} = 37.60$ Å^2, $A_{(110)} = 49.40$ Å^2.

Bond strength: $s_{Ti-O} = 2/3$.

Summations: Σ (101) = 4 x 2/3 x 0.82(θ = 35°) = 2.19, Σ (001) = 1 x 2/3 x 1.00(θ =0°) + 2 x 2/3 x 0.17(θ =80°) = 0.90, Σ (100) = 4 x 2/3 x 0.98(θ = 10°) = 2.67, Σ (110) = 8 x 2/3 x 0.71(θ =45°) = 3.84.

TABLE 9. Cleavability of Octahedrite.

Form	x-ray	{101}	{001}	{100}	{110}
	Dana	{111}	{001}	{110}	{100}
Type		closed bipyramidal	open basal	open prismatic	open prismatic
Number of faces		8	2	4	4
Cleavibility	Calc.	17.2	15.5	13.1	12.9
	Obs.	perfect	perfect	-	-

Brookite

Structure characteristics:[64] Orthorhombic, Γ_o, V_h^{15}. Z = 8

Lattice constants: a = 9.16 Å, b = 5.44 Å, c = 5.14 Å.

Composition: TiO_2. Coordination: Ti-O octahedra.

Areas: $A_{(100)} = 27.96$ Å^2, $A_{(010)} = 47.02$ Å^2, $A_{(001)} = 49.83$ Å^2, $A_{(110)} = 54.80$ Å^2, $A_{(210)} = 73.25$ Å^2, $A_{(111)} = 74.10$ Å^2.

Bond strength: $s_{Ti-O} = 2/3$.

Summations: Σ (210) = 6 x 2/3 x 1.00(Θ =0°) = 4.00, Σ (110) = 3 x 2/3 x 1.00(Θ = 0°) + 3 x 2/3 x 0.70(Θ = 45°) = 3.40, Σ (111) = 14 x 2/3 x 0.70(Θ = 45°) = 6.53, Σ (001) = 10 x 2/3 x 0.70(Θ =45°) = 4.67, Σ (010) = 8 x 2/3 x 0.87(Θ =30°) = 4.64, Σ (100) = 6 x 2/3 x 0.75(Θ =40°) = 3.00.

TABLE 10. Cleavability of Brookite.

Form		x-ray	{210}	{110}	{111}	{001}	{010}	{100}
		Dana	{110}	{120}	{121}	{001}	{010}	{100}
Type			open prismatic	open prism.	closed bipyram.	open basal	open pinacoid.	open pinacoidal
Number of faces			4	4	8	2	2	2
Cleav-ability	Calc.		18.3	16.1	11.0	10.6	10.1	9.3
	Obs.		indistinct	-	-	more indistinct	-	-

Spinel

Structure characteristics: Cubic, Γ_c^1, O_h^7. Z = 8.

Lattice constant: a = 8.09 Å. Composition $MgAl_2O_4$.

Coordination: Mg-O tetrahedra, Al-O octahedra.

Areas: $A_{(100)} = 65.45$ Å^2, $A_{(110)} = 92.28$ Å^2, $A_{(111)} = 15.64$ Å^2.

Bond strengths: $s_{Mg-O} = 1/2$, $s_{Al-O} = 1/2$.

Summations: $\Sigma(111) = 8 \times 1/2 \times 1.00(\Theta = 0°) + 18 \times 1/2 \times 0.71(\Theta = 45°) = 10.39$, $\Sigma(110) = 16 \times 1/2 \times 0.71(\Theta = 45°) + 4 \times 1/2 \times 0.77(\Theta = 40°) = 7.22$, $\Sigma(100) = 8 \times 1/2 \times 1.00(\Theta = 0°) + 4 \times 1/2 \times 0.57(\Theta = 55°) = 5.14$.

TABLE 11. Cleavability of Spinel.

Form		{111}	{110}	{100}
Type		closed octahedral	closed dodecahedral	closed cubic
Number of faces		8	12	6
Cleavability	Calc.	15.3	12.8	12.7
	Obs.	imperfect	-	-

Remark: The reflection surfaces for {111} is poor.

Calcite

Structure characteristics: Trigonal, Γ_{rh}, D_{3d}^6. Z = 2.

Lattice constants: a = 6.36 Å, α = 46°7'. Composition: $CaCO_3$.

Coordination: C-O triangles, Ca-O octahedra.

Areas: $A_{(111)} = 22.02$ Å^2, $A_{(2\bar{1}\bar{1})} = 87.54$ Å^2, $A_{(10\bar{1})} = 151.43$ Å^2, $A_{(211)} = 187.52$ Å^2.

Bond strengths: C-O unbroken, $s_{Ca-O} = 1/3$.

Summations: Σ (211) = 16 x 1/3 x 0.94(θ =20°) = 5.01, Σ (111) = 3 x 1/3 x 0.64(θ =50°) = 0.64, Σ ($2\bar{1}\bar{1}$) = 8 x 1/3 = 0.71(θ=45°) + 4 x 1/3 x 0.64(θ=50°) = 2.75, Σ ($10\bar{1}$) = 24 x 1/3 x 0.77(θ =40°) = 6.16.

TABLE 12. Cleavability of Calcite.

Form	x-ray unit	{211}	{111}	{$2\bar{1}\bar{1}$}	{$10\bar{1}$}
	Dana	{$10\bar{1}1$}	{0001}	{$10\bar{1}0$}	{$11\bar{2}0$}
Type		closed rhombohedral	open basal	open prismatic	open prismatic
Number of faces		6	2	6	6
Cleavability	Calc.	35.4	34.4	31.8	24.6
	Obs.	highly perfect	-	-	-

Remark: Ions of the {211} surface are coplanar.

Phenacite

Structure characteistics: Trigonal, Γ_{rh}, C_{3i}^2. Z = 6.

Lattice constants: a = 7.68 Å, α = 108°1'. Composition: Be_2SiO_4.

Coordination: Be-O tetrahedra, Si-O tetrahedra.

Areas: $A_{(100)} = 56.09$ Å^2, $A_{(2\bar{1}\bar{1})} = 102.21$ Å^2, $A_{(111)} = 134.19$ Å^2, $A_{(10\bar{1})} = 176.82$ Å^2.

Bond strengths: $s_{Si-O} = 1$ (unbroken), $s_{Be-O} = 1/2$.

Summations: Σ (100) = 2 x 1/2 x 0.98(θ =0°) + 2 x 1/2 x 0.57 (θ= 55°) + 1 x 1/2 x 0.71(θ=45°) + 2 x 1/2 x 0.34(θ=70°) + 1 x 1/2 x 0.98 (θ =10°) = 2.74, Σ (111) = 16 x 1/2 x 0.82(θ=35°) = 6.56, $\Sigma(10\bar{1})$ = 12 x 1/2 x 0.98(θ=10°) + 12 x 1/2 x 0.57(θ =55°), $\Sigma(2\bar{1}\bar{1})$ = 4 x 1/2 x 0.57(θ= 55°) + 8 x 1/2 x 0.87(θ=30°) + 2 x 1/2 x 0.77(θ =40°) = 5.39.

TABLE 13. Cleavability of Phenacite.

Form					
	x-ray	{100}	{111}	$\{10\bar{1}\}$	$\{2\bar{1}\bar{1}\}$
	Dana	$\{10\bar{1}1\}$	{0001}	$\{11\bar{2}0\}$	$\{10\bar{1}0\}$
Type		closed rhombohedral	open basal	open prismatic	open prismatic
Number of faces		6	2	6	6
Cleavability	Calc.	20.4	20.4	19.0	18.9
	Obs.	imperfect	-	distinct	-

Remark: According to Niggli[65] {100} very imperfect, {111} perhaps, $\{10\bar{1}\}$ not very distinct.

Kyanite

Structure characteristics:[66,67,68] Triclinic, Γ_{tr} , C_i^1. Z = 4.

Lattice constants: a = 7.09 Å, b = 7.72 Å, c = 5.56 Å.

α = 90°5.5', β = 101°2', γ = 105°44.5'.

Composition: Al_2OSiO_4. Coordination: Al-O octahedra, Si-O tetrahedra.

Areas: $A_{(010)} = 38.64$ Å^2, $A_{(100)} = 42.90$ Å^2, $A_{(001)} = 53.54$ Å^2.

Bond strengths: $s_{Si-O} = 1$ (unbroken), $s_{Al-O} = 1/2$.

Summations: Σ (100) = 8 x 1/2 x 0.71($\Theta \approx 45°$) = 2.84, Σ (010) =

6 x 1/2 x 0.98($\Theta \approx 10°$) + 4 x 1/2 x 0.17($\Theta \approx 80°$) = 3.28,

Σ (001) = 4 x 1/2 x 0.26($\Theta \approx 75°$) + 4 x 1/2 x 0.71($\Theta \approx 45°$) +

6 x 1/2 x 0.87($\Theta \approx 30°$) = 4.55.

TABLE 14. Cleavability of Kyanite.

Form		{100}	{010}	{001}
Type		open pinacoidal	open pinacoidal	open basal
Number of faces		2	2	2
Cleavability	Calc.	15.1	11.7	11.7
	Obs.	very perfect	less perfect	-

Remarks: Ions of the {100} surface are coplanar. Parting // {001} .

Topaz

Structure characteristics:[69,70] Orthorhombic, Γ_o, V_h^{16}. Z = 4.

Lattice constants: a = 4.64 Å, b = 8.78 Å, c = 8.37 Å.

Composition: $Al_2SiO_4F_2$.

Coordination: Si-O tetrahedra, Al-O octahedra.

Areas: $A_{(010)} = 38.84$ Å^2, $A_{(001)} = 40.74$ Å^2, $A_{(100)} = 73.48$ Å^2, $A_{(110)} = 83.12$ Å^2.

Bond strengths: $s_{Si-O} = 1$(unbroken); $s_{Al-O} = 1/2$, $s_{Al-F} = 1/2$, $s_{Al-O} = 1/4$.

Summations: Σ (001) = 4 x 1/2 x 0.71(Θ=45°) = 1.42, Σ (100) = 8 x 1/2 x 0.65(Θ=50°) + 4 x 1/4 x 0.71(Θ=45°) = 3.27, Σ (010) = 4 x 1/2 x 0.71(Θ=45°) + 4 x 1/4 x 0.71(Θ=45°) = 2.13, Σ (110) = 3 x 1/2 x 1.00(Θ=0°) + 8 x 1/2 x 0.71(Θ=45°) + 4 x 1/4 x 0.71(Θ=45°) = 5.05.

TABLE 15. Cleavability of Topaz.

Form		{001}	{100}	{010}	{110}
Type		open basal	open pinacoidal	open pinacoidal	open prismatic
Number of Faces		2	2	2	4
Cleavability	Calc.	28.6	22.4	18.1	16.4
	Obs.	highly perfect	-	-	-

Remark: Ions of {001} surface are coplanar.

Zircon

Structure characteristics: Tetragonal, Γ_t', D_{4h}^{19}. Z = 4.

Lattice constants: a = 6.58 Å, c = 5.93 Å. Composition: $ZrSiO_4$.

Coordination: Si-O tetrahedra, Zr-O hexahedra.

Areas: $A_{(100)} = 39.02$ Å^2, $A_{(001)} = 43.30$ Å^2, $A_{(110)} = 55.15$ Å^2, $A_{(101)} = 58.30$ Å^2, $A_{(111)} = 70.14$ Å^2.

Bond strengths: $s_{Si-O} = 1$ (unbroken), $s_{Zr-O} = 1/2$.

Summations: Σ (100) = 4 x 1/2 x 0.98(Θ =10°) = 1.96, Σ (110) = 8 x 1/2 x 0.71(Θ=45°) = 2.84, Σ (101) = 4 x 1/2 x 0.71(Θ=45°) + 8 x 1/2 x 0.64 (Θ=50°) = 3.98, Σ (001) = 8 x 1.2 x 0.85(Θ=32°) + 4 x 1/2 x 0.14(Θ=82°) = 3.68, Σ (111) = 8 x 1/2 x 0.82(Θ=35°) + 8 x 1/2 x 0.71(Θ=70°) + 6 x 1/2 x 0.34(Θ=70°) = 7.14.

TABLE 16. Cleavability of Zircon

Form		{100}	{110}	{101}	{001}	{111}
x-ray		{100}	{110}	{101}	{001}	{111}
Dana		{110}	{100}	{111}	{001}	{221}
Type		open prismatic	open prismatic	closed bipyram.	open basal	closed bipyramidal
Number of faces		4	4	8	2	8
Cleavability	Calc.	19.9	19.4	14.6	11.7	9.8
	Obs.	imperfect	-	less distinct	-	-

Grossularite

Structure characteristics: Cubic, $\Gamma_c^{\prime\prime}$, O_h^{10}. Z = 8.

Lattice constant: a = 11.83 Å. Composition: $Ca_3Al_2(SiO_4)_3$.

Coordination: Si-O tetrahedra, Al-O octahedra, Ca-O hexahedra.

Areas: $A_{(100)} = 139.95$ Å^2, $A_{(110)} = 197.90$ Å^2, $A_{(111)} = 242.5$ Å^2.

Bond strengths: $s_{Si-O} = 1$ (unbroken), $s_{Al-O} = 1/2$, $s_{Ca-O} = 1/4$.

Summations: Σ (110) = 4 x 1/2 x 0.98(Θ =10°) + 8 x 1/2 x 0.71(Θ = 45°) + 8 x 1/2 x 0.26(Θ =75°) + 12 x 1/4 x 0.71(Θ = 45°) + 4 x 1/4 x 0.87(Θ = 30°) = 8.84, Σ (100) $\neq$ 8 x 1/2 x 0.94(Θ =20°) + 8 x 1/2 x 0.26(Θ = 75°) + 8 x 1.4 x 0.87(Θ =30°) + 8 x 1/4 x 0.98(Θ =10°) = 8.50.

TABLE 17. Cleavability of Grossularite.

Form		{110}	{100}	{111}
Type		closed dodecahedral	closed cubic	closed octahedral
Number of faces		12	6	8
Cleavability	Calc.	22.4	16.5	probably less than {100}
	Obs.	sometimes rather distinct	-	-

Remarks: It is uncertain whether {110} is cleavage or parting. The limit of error for the calculated {111} cleavability value is large.

Melilite

Structure characteristics:[71] Tetragonal, Γ_t, D^3_{2d}. Z = 2.

Lattice constants: a = 7.73 Å, c = 5.01 Å.

Composition: $(Ca,Na)_2(Mg,Al)_1(Si,Al)_2O_7$.

Coordination: Si-O tetrahedra, Mg-O tetrahedra, Ca-O hexahedra.

Areas: $A_{(100)} = 38.73$ Å^2, $A_{(110)} = 54.76$ Å^2, $A_{(001)} = 59.74$ Å^2,

Bond strengths: $s_{Si-O} = 1$ (unbroken), $s_{Mg-O} = 1/2$, $s_{Ca-O} = 1/4$.

Summation: Σ (001) = 16 x 1/4 x 0.42(Θ =65°) = 1.68, Σ (110) = 2 x 1/2 x 0.17(Θ =80°) + 2 x 1/2 x 0.91(Θ =25°) + 4 x 1/4 x 0.64(Θ=50°) + 2 x 1/4 x 0.71(Θ =45°) = 2.07, Σ (100) = 2 x 1/2 x 0.91(Θ = 25°) + 8 x 1/4 x 0.64(Θ =50°) = 2.19.

TABLE 18. Cleavability of Melilite.

Form	x-ray	{001}	{110}	{100}
	Dana	{001}	{100}	{110}
Type		open basal	open prismatic	open prismatic
Number of faces		2	4	4
Cleavability	Calc.	35.5	26.5	17.6
	Obs.	distinct	indistinct	-

Remark: Ions of the {001} surface are coplanar.

Diopside

Structure characteristics:[72] Monoclinic, Γ_m^1, C_{2h}^6 Z = 4.

Lattice constants: a = 9.71 Å, b = 8.89 Å, c = 5.24 Å, β = 74°10'.

Composition: $CaMgSi_2O_6$.

Coordination: Si-O tetrahedra, Mg-O octahedra, Ca-O hexahedra.

Areas: $A_{(100)} = 46.58$ Å^2, $A_{(010)} = 48.84$ Å^2, $A_{(110)} = 67.50$ Å^2, $A_{(001)} = 86.33$ Å^2.

Bond strengths: $s_{Si-O} = 1$ (unbroken for {100} and {110}), $s_{Mg-O} = 1/3$, $s_{Ca-O} = 1/4$.

Summations: Σ (110) $\doteqdot$ 8 x 1/3 x 0.64(Θ = 50°) + 8 x 1/4 x 0.50(Θ = 60°) + 4 x 1/4 x 0.94(Θ = 20°) = 3.64, Σ (001) = 4 x 1 x 0.87(Θ = 30°) + 2 x 1/3 x 0.98(Θ = 10°) + 4 x 1/4 x 0.71(Θ = 45°) = 4.85, Σ (100) = 6 x 1/3 x 0.71(Θ = 45°) + 2 x 1/4 x 0.64(Θ = 50°) + 2 x 1/4 x 0.50(Θ = 60°) + 4 x 1/4 x 0.71(Θ = 45°) = 2.70, Σ (010) = 4 x 1 x 0.34(Θ = 70°) + 4 x 1/3 x 0.71(Θ = 45°) + 4 x 1/4 x 0.71(Θ 45°) = 3.02.

Table 19. Cleavability of Diopside.

Form		{110}	{001}	{100}	{010}
Type		open prismatic	open basal	open pinacoidal	open pinacoidal
Number of faces		4	2	2	2
Cleavability	Calc.	18.5	17.8	17.2	16.3
	Obs.	rather perfect (sometimes) but interrupted	-	-	-

Remarks: {110} often only observed in thin sections $\perp$ c. Parting on {001} often very prominent, on {100} less distinct and less common.

Tremolite

Structure characteristics:[73] Monoclinic, Γ_m^1 (oriented as a body centered lattice in order to agree with the usual crystallographic axes), C_{2h}^3, Z = 2.

Lattice constants: a = 9.~~87~~[78] Å, b = 17.8 Å, c = 5.26 Å, β = 73°58'.

Composition: $Ca_2Mg_5(Si_4O_{11})_2(OH)_2$.

Coordination: Si-O tetrahedra, Mg-O octahedra, Ca-O hexahedra.

Areas: $A_{(010)} = 49.38$ Å^2, $A_{(100)} = 93.63$ Å^2, $A_{(110)} = 104.60$ Å^2, $A_{(001)} = 174.08$ Å^2.

Bond strengths: $s_{Si-O} = 1$ (unbroken for {110}, {100} and {010})

$s_{Mg-O} = 1/3$, $s_{Mg-OH} = 1/2$ $s_{Mg-O} = 1/6$, $s_{Ca-O} = 1/4$.

Summations: Σ (110) = 12 x 1/4 x 0.64(Θ=50°) + 4 x 1/3 x 0.34(Θ=70°) = 2.37, Σ (100) = 12 x 1/4 x 0.64(Θ=50°) + 4 x 1/3 x 0.34(Θ=70°) = 2.37, Σ (010) = 4 x 1/3 x 0.71(Θ=45°) + 4 x 1/4 x 0.64(Θ=50°) = 1.59, Σ (001) = 8 x 1 x 1.00(Θ=0°) + 8 x 1/4 x 0.64(Θ=50°) + 4 x 1/3 x 0.87(Θ=30°) + 2 x 1/6 x 0.87(Θ=30°) = 10.73.

TABLE 20. Cleavability of Tremolite.

Form		{110}	{100}	{010}	{001}
Type		open prismatic	open pinacoidal	open pinacoidal	open basal
Number of faces		4	2	2	2
Cleavability	Calc.	44.1	39.5	31.0	16.6
	Obs.	highly perfect	sometimes distinct	sometimes distinct	-

Remarks: See discussion.

Muscovite

Structure characteristics:[74,75,76] Monoclinic, Γ_m^1, C_{2h}^6. Z = 4.

Lattice constants: a = 5.19 Å, b = 9.00 Å, c = 20.04 Å, $\beta = 95°30'$.

Composition: $KAl_2(Si_3Al)O_{10}(OH,F)_2$.

Coordination: Si,Al-O tetrahedra, Al-(O,OH) octahedra; $V_K = 12$.

Areas: $A_{(001)} = 46.8$ Å^2, $A_{(010)} = 103.0$ Å^2, $A_{(100)} = 180.0$ Å^2.

Bond strengths: $s_{Si-O} = 1$ (unbroken), s_{Al-O}(tetrahedron) = 3/4, s_{Al-O}(octahedron) = 1/2, $s_{Al-(OH,F)} = 1/2$, $s_{Al-O} = 1/4$, $s_{K-O} = 1/12$.

Summations: Σ (001) = 12 x 1/12 x 0.64(Θ =50°) = 0.64, Σ (100) = 6 x 3/4 x 0.71(Θ =45°) + 8 x 1/2 x 0.71(Θ =45°) + 8 x 1/4 x 0.57(Θ =55°) = 7.18, Σ (010) = 3 x 3/4 x 1.00(Θ =0°) + 4 x 1/2 x 0.71(Θ =45°) + 8 x 1/4 x 0.57(Θ =55°) = 4.81.

TABLE 21. Cleavability of Muscovite.

Form				
Form	x-ray	{001}	{100}	{010}
	Dana	{001}	{201}	{010}
Type		open basal	open pinacoidal	open pinacoidal
Number of faces		2	2	2
Cleavability	Calc.	73.1	25.0	21.4
	Obs.	eminent	-	-

Remark: Fourier analysis indicates that the ions of the separation surfaces for {001} are exactly coplanar.

Sodalite

Structure characteristics:[77,78] Cubic, Γ_c (closely approximates a body-centered lattice), T_d^4 (possibly T_d^1). Z = 2.

Lattice constant: a = 8.87 Å. Composition: $Na_4Al_3Si_3O_{12}Cl$.

Coordination: Si-O tetrahedra, Al-O tetrahedra, Na-O hexahedra.

Areas: $A_{(100)} = 78.68$ Å^2, $A_{(110)} = 108.72$ Å^2, $A_{(111)} = 136.12$ Å^2.

Bond strengths: $s_{Si-O} = 1$ (unbroken), $s_{Al-O} = 3/4$, $s_{Na-O} = 1/8$.

Summations: Σ (110) = 4 x 3/4 x 0.71(θ =45°) + 2 x 1/8 x 0.71(θ =45°) + 2 x 1/8 x 0.34(θ =70°) = 2.39, Σ (100) = 2 x 3/4 x 0.77(θ =40°) + 2 x 3/4 x 0.71(θ =45°) + 4 x 1/8 x 0.34(θ =70°) = 2.40, Σ (111) = 4 x 3/4 x 0.87(θ =30°) + 2 x 3/4 x 0.98(θ =10°) + 1 x 1/8 x 1.00(θ =0°) = 4.21.

TABLE 22. Cleavability of Sodalite.

Form		{110}	{100}	{111}
Type		closed dodecahedral	closed cubic	closed octahedral
Number of faces		12	6	8
Cleavability	Calc.	45.5	32.7	32.2
	Obs.	more or less distinct	-	-

6. Discussion of Cleavage.

Comparative cleavabilities and data on the cohesive properties of the ionic minerals studied are given in Table 23. The twenty-five minerals listed are arranged in the order of their highest cleavability. The calculated cleavabilities for the different forms, taken from the foregoing tables, are contained in the second column, observed cleavage being denoted by underlines, three for very good, two for good, and one for poor. The table shows that the general agreement between calculated cleavability values and observed cleavage is good.

The best observed cleavage for each species is for the form with the highest calculated cleavability value, except those of fluorite, lime, periclase and bromellite. These anomalies are probably due to the neglect of angular change in Θ during the process of rupture; since the treatment is in the nature of a first order approximation it is to be expected that such cases may occur. In the case of fluorite there may exist the additional effect of a good reflecting surface for a form of lower cleavability in the sequence. The lack of observed cleavage for cristobalite and corundum is discussed later (see Table 24). Second order effects due to impurities, growth conditions and mechanical strain such as gliding set up during the process of cleavage although difficult to evaluate do not seem to materially affect the results.

The agreement of muscovite is excellent; its high cleavability is due to the comparatively weak K-O bonds which hold strong layers together; the statistical alternation of K^+ ions across the cleavage surface results in electrical neutrality. An extreme case of this nature is that of talc whose structure consists of neutral layers held together by second order electrical effects; since there are no direct

TABLE 23. Comparative Cleavabilities and Cohesive Properties of Ionic Minerals.

Species	Sequence of cleavabilities				Total no. of planes	Hardness	Fracture	Tenacity
Muscovite	73.1	25.0	21.4		6	2.00-2.25	-	-
Sodalite	45.5	32.7	33.2		26	5.50-600	uneven to subc.	Brittle
Tremolite	44.1	39.5	31.0	16.6	10	5.00-6.00	"	Brittle
Melilite	35.5	26.5	17.6		10	5.00	uneven to conch.	Brittle
Calcite	35.4	34.4	31.8	24.6	20	3.00	conch. (with dif.)	-
Villiaumite	31.5	31.5*	22.3		26	< 3.00	-	-
Sellaite	30.1	30.1	23.2	16.7	18	5.00-6.00	conchoidal	Brittle
Fluorite	29.7*	25.7	25.7*		26	4.00	flat-conch.	Brittle
Topaz	28.6	22.4	18.1	16.4	10	8.00	uneven to subc.	Brittle
Grossularite	22.4	16.5			18	6.50-7.50	"	Brittle
Cristobalite	22.2	22.0	21.9		26	6.00-7.00	-	-
Tridymite	22.0	21.9	20.6	20.4	26	7.00	conchoidal	Brittle
Phenacite	20.4	20.4	19.0	18.9	20	7.50-8.00	conchoidal	Brittle
Zircon	19.9	19.4	14.6?	11.7 9.8	26	7.50	conchoidal	Brittle
Quartz	18.7	17.4	17.0	16.2	26	7.00	subc. to conch.	Brittle
Diopside	18.5	17.8	17.2	16.3	12	5.00-6.00	uneven to conch.	Brittle
Brookite	18.3	16.1	11.0 10.1	10.6? 9.3	22	5.50-6.00	subconch.	Brittle
Octahedrite	17.2	15.5	13.1	12.9	18	5.50-6.00	subconch.	Brittle
Lime	17.2	17.2*	12.1		26	-	-	-
Spinel	15.3	12.8	12.7		26	8.00	conchoidal	Brittle
Kyanite	15.1	11.7	11.7		6	5.00-7.25	-	-
Rutile	14.4	14.4	11.1	8.1?	18	6.00-6.50	uneven to subc.	Brittle
Periclase	13.2	13.2*	9.3		26	6.00	-	-
Bromellite	12.5	12.5*	11.7	11.1	26	9.00	-	-
Corundum	12.4	10.2	9.5	9.2 8.6	26	9.00	uneven to conch.	Brittle

Note: Observed cleavage is denoted by underlining.
≡ very good = good — poor.

bonds the cleavability value is very high. In the case of diopside although there are single chains of Si-O tetrahedra parallel to the c-axis the numerical values for the possible cleavage forms are fairly close together indicating a compact structure (see Table 24); this is confirmed by the observed frequent failure of the prismatic {110} cleavage except in thin section. Tremolite with double chains of tetrahedra gives an interesting contrast. The high cleavability (44.1) for {110} together with the low cleavability (16.6) for {001} clearly indicates a structure capable of yielding fibres; the probable cleavage path for {110} is shown in Figure 2; a suggested[79] cleavage giving the very low value of 15.9 for the cleavability of {110} is erroneous, if the calculations of this paper are trustworthy. The cleavage of that portion of the path shown in the figure parallel to b is analogous to the mica {001} cleavage with its accompanying high cleavability; since two double Si-O chains are held together by strong Mg-O bonds the resulting columnar units have nearly square cross-section of greatly increased strength. The silica modifications, namely quartz, cristobalite and tridymite, have their cleavabilities calculated from the high temperature forms since it is probable that these configurations are approximate to those of the low temperature forms; the agreement obtained is good; the compact structures indicated by their cleavabilities is reflected in the poor or no cleavage (see Table 24). Sellaite, rutile and octahedrite give excellent agreement. The form {111} of spinel has the highest cleavability but probably due to a poor reflecting surface the observed cleavage instead of being good is imperfect; this is in marked contrast to the effect of surface on the {211} form of calcite (see Table 25). The agreement of kyanite, topaz and melilite

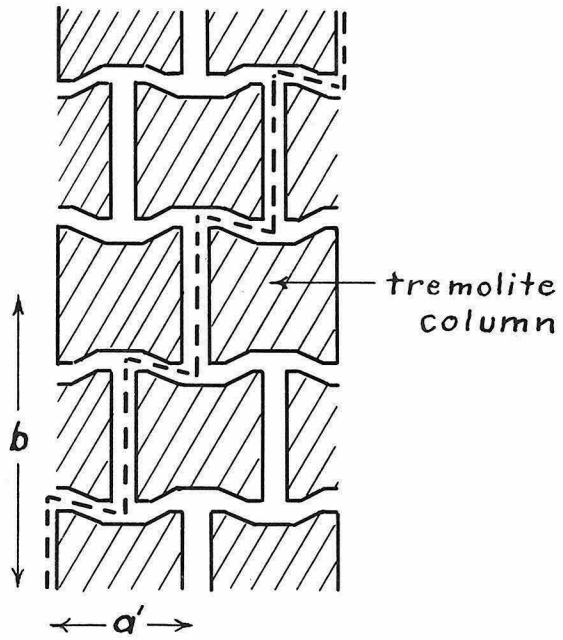

Figure 2.

Basal projection of tremolite columns.

The {110} cleavage path is indicated.

is excellent. Sodalite, a mineral with a three-dimensional network of tetrahedra, gives very good agreement. It is seen that the cleavage of a mineral is predominately determined by the relative magnitude of the calculated cleavabilities for the crystal. In species where pronounced cleavage occurs the calculated cleavability value for that form is appreciably greater than the values for other forms of the same crystal; an example is furnished by muscovite whose eminent {001} cleavage has a cleavability 200% greater than that of any other form. That the change in observed cleavage from mineral to mineral is not determined by the relative values of the highest calculated cleavabilities is shown by the form {110} of tremolite having the same cleavability as {110} of sodalite while the observed cleavage for tremolite is highly perfect in marked contrast to the more or less distinct cleavage of sodalite.

If the cleavabilities for a large number of forms were calculated, it is probable that the values would approach an asymptotic lower limit. Such a tendency is shown by the data of Table 23 as for example in the cases of brookite whose last form calculated values are 11.0, 10.6, 10.1, 9.3 and corundum whth values of 10.2, 9.5, 9.2, 8.6. Since the cleavability range of a mineral is the interval between the greatest and least of its cleavabilities, these may be replaced by the greatest and least of the calculated values and the approximate range so obtained may be designated as the "range of cleavability values." The lower asymptotic limit being unknown, the significance of this range is to some extent determined by the total number of planes in the forms considered. This number is given in the third column. There seems to be a correlation between the number of planes in a form and the degree

TABLE 24. Restricted Range of Cleavability Values and Cleavage.

Species	Number of Planes	Range of Cleavability Values	Cleavage
Cristobalite	26	22.2-21.9	None
Tridymite	26	22.0-20.4	Not distinct
Phenacite	20	20.4-18.9	Poor
Quartz	26	18.7-16.2	Difficult
Diopside	12	18.5-16.3	Often only in thin section
Spinel	26	15.3-12.7	Poor
Bromellite	26	12.5-11.1	Doubtful
Corundum	26	12.4-8.6	None

of cleavage as evidenced by the excellent cleavage of muscovite, topaz and kyanite, each having two planes in the cleavage form while sodalite and grossularite with twelve planes for {110} have poor cleavage.

It follows that minerals having a restricted range of cleavability values should not show pronounced cleavage on any form. As shown by the minerals listed in Table 24, this is in agreement with the results of observation. The cleavability values given in column three for the forms considered change by only a few percent. Cristobalite and corundum show no cleavage, while for tridymite, phenacite, quartz, etc., the reported cleavage is poor.

The observational data on hardness (according to the scale of Mohs) is given in column four of table 23. It is noteworthy that the difference in cleavability between the two end species muscovite and corundum is large, the former having six times the cleavability of the latter, and is correlative with the least and greatest of the hardness values, and further that in a general way the intermediate cleavability and hardness values tend to be inverse to each other. These data suggest that hardness increases as the cleavability decreases. To establish the exact nature of this inverse relationship requires more detailed work.

Departure of the rupture surface from a planar condition with its accompanying good cleavage results in the irregular surface of the conchoidal fracture. As indicated by columns five and six of Table 23, the observed fracture range is uneven to conchoidal with the tenacity uniformly brittle.

The relatively less important component of cleavage is the effect of the optical properties of the cleavage surface. There are listed in Table 25 mineral species whose highest calculated cleavabilities

TABLE 25. Effect of Plane Optical Surface on Cleavage

Species	Cleavage form	Cleavability	Surface	Cleavage
Muscovite	{001}	73.1	Exactly plane	Eminent
Calcite	{211}	35.4	Plane	Highly perfect
Villiaumite	{100}	31.5	Plane	Complete
Topaz	{001}	28.6	Plane	Highly perfect
Lime	{100}	17.2	Plane	Complete
Kyanite	{100}	15.1	Plane	Very perfect
Periclase	{100}	13.2	Plane	Perfect

range from 73.1 (muscovite) to 13.2 (periclase), being the maximum and nearly the minimum of Table 23. All these cleavage forms have planar surfaces, with that of muscovite known to be exactly so. In strong contrast to the variation in cleavability, the degree of cleavage given in the last column of the table is observed to be much better than average. It is evident that the sequence of cleavabilities for a species need not be the same as that of observed cleavage (cleavability plus optical effect) although in general they correspond.

The cleavabilities of parting forms for grossularite, tridymite, diopside and corundum are given in Table 26. Comparison of the data of coumns three and four show that the cleavabilities for these forms are at or near the maximum limit of the range of cleavability values, indicating that cleavage may frequently occur on such forms rather than parting.

The use of Equation 16 gives not only calculated cleavabilities for various forms of the same species but also permits comparing cleavabilities of different minerals. Although restricted in this study to ionic minerals it is probable that the expression for cleavability is of more general scope.

TABLE 26. Cleavability and Parting.

Species	Form	Cleavability	Range of cleavability values of species	Observation
Grossularite	{110}	22.4	22.4 - 16.5	Uncertain if cleavage or parting
Tridymite	{0001}	21.9	22.0 - 20.4	Parting sometimes observed
Diopside	{001}	17.8	18.5-16.3	Parting often very prominent
Corundum	{110}	12.4	12.4 - 8.6	Parting often prominent

7. Conclusions

1. The dominant component of the phenomenon of mineral cleavage is cleavability.
2. Ionic cleavability is given by the expression

$$C_{\{hkl\}} = \frac{A_{(khl)}}{\sum_i n_i \, s_i \cos \Theta_i}.$$

3. A limited range of cleavability values indicates absence of cleavage.
4. The higher degrees of cleavage are due to high relative cleavability plus plane optical surfaces.
5. The data suggest that hardness increases as cleavability decreases.
6. High relative cleavabilities for parting forms indicate cleavage rather than parting.

Balch Graduate School of the Geological Sciences,
California Institute of Technology.

BIBLIOGRAPHY

1. Dana, J.D., (Sixth ed. by E.S.Dana)
"System of Mineralogy" Wiley, New York (1892).

2. Tertsch, H. "Einfache Kohäsionsversuche I, II, III."
Z.Krist., 74, 476-500 (1930); 78, 53-75 (1931);
81, 264-274 (1932).

3. Bravais, A. "Etudes Cristallographiques."
Jour.d.l'Ecole Poly., 22, 101-278 (1851).

4. Sohncke, L. "Ueber Spaltungsflächen und naturliche Kristallflächen."
Z.Krist., 13, 214-235 (1887).

5. Tertsch, H. "Spaltbarkeit und Struktur im trigonalen und
hexagonalen Systeme." Z.Krist., 47, 56-74 (1909).

6. Ewald, P.P. and Friedrich, W. "Röntgenaufnahmen von kubischen
Kristallen, insbesondere Pyrit." Ann.d.Phys., 44, 1183-1184 (1914)

7. Stark, J. "Neure Ansichten über die zwischen- und
innermolekulare Bindung in Kristallen."
Jahrb. der Rad. u.Elek., 12, 279-296 (1915).

8. Scharizer, R. "Die Bragg'schen Kristallgitter und die
Spaltbarkeit." Z.Krist., 55, 440-443 (1916).

9. Niggli, P. "Geometrische Kristallographie des Diskontinuums."
Borntraeger, Leipzig. (1919).

10. Beckenkamp, J. "Atomanordung und Spaltbarkeit."
Z.Krist., 58, 7-39 (1923).

11. Parker, R.L. "Zur Kristallographie von Anatase und Rutile.
II. Teil. Die Anatasstruktur." Z.Krist., 59, 1-54 (1923).

12. Barlow, W. "Geometrische Untersuchung über eine mechanische
Ursuche der Hamogenität der Struktur und der Symmetrie."
Zeit.Krist., 29, 433-588 (1898).

13. Ewald, P.P. "Die Intensität der Interferenzflecke bei Zinckblende
und das Gitter der Zinkblende." Ann.der Phys., 44, 257-282 (1914)

14. See Ref. 6.

15. Huggins, M.L. "Crystal Cleavage and Crystal Structure"
Amer.Jour.Sci., 5, 303-313 (1923).

16. Tertsch, H. "Bemerkungen zur Spaltbarkeit."
Z.Krist., 65, 712-718 (1927).

17. Pauling, L. "The Structure of Some Sodium and Calcium Aluminosilicates." Proc.Nat.Acad.Sci., 16, 453-459 (1930).

18. Tertsch, H. "Wie erfolgt der Spaltungsvorgang bie Kristallen?" Z.Krist., 81, 275-284 (1932).

19. Gibbs, J.W. "On the Equilibrium of Heterogeneous Substances." (1876) Collected Works. Longmans, New York (1928).

20. Lewis and Randall, "Thermodynamics." McGraw-Hill, New York (1923).

21. Condon and Morse. "Wave Mechanics." McGraw-Hill, New York (1929).

22. Unsöld, A. "Beitrage zur Quantenmechanik der Atome." Ann.der Phys., 82, 355-393 (1927).

23. Pauling, L. "The Sizes of Ions and the Structure of Ionic Crystals." J.Am.Chem.Soc., 49, 765-790 (1927).

24. Jeans, J.H. "The Mathematical Theory of Electricity and Magnetism." 5th ed. University Press, Cambridge (1925).

25. Around 1% or about 2 large calories per mole for crystals of the halite type.

26. Born, M. "Atomtheorie des Festen zustandes." Eney.d.Math.Wiss., 5, 527-789. Teubner, Leipzig (1923).

27. Born, M. and Bollnow, O.F. "Der Aufbau der festen Materie" Hdbk.d.Phy., 24, 370-465. Springer, Berlin (1927).

28. See Ref. 13

29. See Ref. 24.

30. Langmuir, I. "The Constitution and Fundamental Properties of Solids and Liquids." J.Am.Chem.Soc., 38, 2221-2295 (1916).

31. Harkins, W.D. et al. "The Structure of the Surfaces of Liquids, etc." J.Am.Chem.Soc., 39, 354-364 (1917).

32. Born, M. and Stern, O. "Über die Oberflachenenergie der Kristalle und ihren Einfluss auf die Kristallgestalt." Sitzber.d.Pr.Akad.d.Wiss., Berlin. 1919, 910-913.

33. Harkins, W.D. and Cheng, Y.C. "The Orientation of Molecules in Surfaces." J.Am.Chem.Soc., 43, 35-53 (1921).

34. Lennard-Jones, J.E. In Fowler, R.H. "Statistical Mechanics." Univ.Press, Cambridge (1929).

35. See Ref. 19.

36. Curie, P. "Sur la formation des cristaux et sur les constantes capillaires de leurs différentes faces." Bull.Soc.Miner.Fr., 8, 145-150 (1885).

37. Ehrenfest, P. "Zur Kapillaritätstheorie der Kristallgestalt." Ann.der Phy., 48, 360-368 (1915).

38. See Ref. 19.

39. Bakker, G. "Kapillarität und Oberflächenspannung." Hdbk.d.Exper.Phy., Vol.VI, Akad.verlags, Leipzig (1928).

40. Adams, N.K. "The Physics and Chemistry of Surfaces." Clarendon Press, Oxford (1930).

41. Wulff, G. "Zur Frage der Geschwindigkeit der Wachstums und der Auflösung der Kristallflächen." Z.Krist., 34, 449-530 (1901).

42. Hilton, H. "Mathematical Crystallography." Clarendon Press, Oxford (1903).

43. Yamada, M. "Über de Oberflächenenergie der Kristalle und die Kristallformen." Phy.Zeit., 24, 364-372 (1923).

44. Yamada, M."Anhang ... " Phy.Zeit. 25, 52-56 (1924).

45. Biemuller, J. "Über die Oberflächenenergie der Alkalihalogenide." Zeit.f.Phy., 38, 759-771 (1926).

46. Usually coinciding with the center of symmetry.

47. Griffith, A.A. "The Phenomena of Rupture and Flow in Solids." Trans.Roy.Soc., London, A 221, 163-198 (1924).

48. Polanyi, M. "Über die Natur der Zerreissvorganges." Zeit.f.Phys., 7, 323-327 (1921).

49. See Ref. 30.

50. See Ref. 31.

51. Smekal, A. "Kohäsion der Festkörper." In Auerbach und Hort. Hdbk.d.phy.u.tech.Mechanik, 42, 1-153 (1931).

52. Pauling, L. "The Principles Determining the Structure of Complex Ionic Crystals." J.Am.Chem.Soc., 51, 1010-1026 (1929).

53. For a physical justification of the electrostatic valence bond see Bragg, W.L. "The Architecture of the Solid State." (Kelvin Lecture) Nature, 128, 210-212, 248-250 (1931).

54. Washington, H.S. "Chemistry of the Earth's Crust." Jour.Franklin Inst., 190, 757-815 (1920).

55. Niggli, P. "Ore Deposition of Magmatic Origin." Murby, London, (1929).

56. Goldschmidt, V.M. "Geochemische Verteilungsgesetze und kosmische Häufigkeit der Elemente." Naturw. 18, 999-1013 (1930).

57. Bragg, W.L. "The Structure of the Silicates" Z.Krist., 74, 237-305 (1930).

58. Nára-Szabo, St. "Ein auf der Kristallstruktur basierendes Silicatsystem." Z.Phy.Chem., 9 B, 356-377 (1930).

59. Hintze, C. "Handbuch der Mineralogie." Veit, Leipzig (1915).

60. Groth, P. "Chemische Kristallographie." Engelmann, Leipzig (1906).

61. Aminoff, G. "Über Berylliumoxyd als Mineral und dessen Kristallstruktur." Z.Krist., 62, 113-122 (1925); 63, 175 (1926).

62. See Ref. 59.

63. Rogers, A.F. "Cleavage and Parting in Quartz." (Abstract) Amer.Miner., 18, 111-112 (1933).

64. Pauling, L. and Sturdivant, J.H. "The Crystal Structure of Brookite." Z.Krist., 68, 239-256 (1928).

65. Niggli, P. "Lehrbuch der Mineralogie." 2nd ed. Vol.II. Borntraeger, Berlin (1926).

66. Bragg, W.L. and West, J. "The Structure of Certain Silicates." Proc.Roy.Soc., A 114, 450-473 (1927).

67. See Ref. 52.

68. Náray-Szabo, S., Taylor, W.H. and Jackson, W.W. "The Structure of Cyanite." Z.Krist., 71, 117-130 (1929).

69. Pauling, L. "The Crystal Structure of Topaz." Proc.Nat.Acad.Sci., 14, 603-606 (1928).

70. Alston, N.A. and West, J. "The Structure of Topaz." Z.Krist., 69, 149-167 (1928).

71. Warren, B.E. "The Structure of Melilite ... " Zeit.Krist., 74, 131-138 (1930).

72. Warren, B. and Bragg, W.L. "The Structure of Diopside, ... " Z.Krist., 69, 168-193 (1928).

73. Warren, B.E. "The Structure of Tremolite ... " Z.Krist., 72, 42-57 (1929).

74. Mauguin, C. "Étude du mica muscovite au moyen rayons X." Comp.Rend., 185, 288-291 (1927).

75. Pauling. L. "The Structure of the Micas and Related Minerals." Proc.Nat.Acad.Sci., 16, 123-129 (1930).

76. Jackson, W.W. and West J. "The Crystal Structure of Muscovite ..." Z.Krist., 76, 211-227 (1931).

77. Pauling L. "The Structure of Sodalite ..." Z.Krist., 74, 213-225 (1930).

78. Barth, T.F. "The Structures of the Minerals of the Sodalite Family." Z.Krist., 83, 405-414 (1932).

79. See Ref. 73.

ACKNOWLEDGMENT

This research was greatly aided by a Storrow Fellowship in Geology of the National Research Council. I wish to thank Professor Linus Pauling for his kindly interest and advice throughout the investigation. I am also indebted to the Gates Chemical Laboratory for research facilities.

Reprint from „Zeitschrift für Kristallographie". Bd. 75, Heft 1/2.
Akademische Verlagsgesellschaft m. b. H. in Leipzig, 1930.

The Crystal Structure of Bixbyite and the *C*-Modification of the Sesquioxides.

By

Linus Pauling and **M. D. Shappell** in Pasadena.

Gates Chemical Laboratory, California Institute of Technology, Pasadena, California. Communication No. 259.

(With six figures.)

1. Introduction.

It was discovered in 1925 by Goldschmidt[1]) that an extensive series of sesquioxides form cubic crystals with the unit of structure containing $16\,M_2O_3$, the value of a varying between 9.3 Å and 10.9 Å. An atomic arrangement based on the space group T^5 was assigned this C-modification of the sesquioxides by Zachariasen[2]), who studied crystals of Sc_2O_3, Mn_2O_3, Y_2O_3, In_2O_3, Tl_2O_3, Sm_2O_3, Eu_2O_3, Gd_2O_3, Tb_2O_3, Dy_2O_3, Ho_2O_3, Er_2O_3, Tm_2O_3, Yb_2O_3, Lu_2O_3, and the mineral bixbyite, $(Fe, Mn)_2O_3$. Zachariasen's procedure was the following. Using data from powder and Laue photographs of Tl_2O_3, and neglecting the contribution of the oxygen atoms to the reflections, he decided that the space group is T^5, with the $32\,Tl$ in $8\,b$ with parameter $t = 0.25$, in $12\,c$ with parameter $u = 0.021$, and in $12\,c$ with parameter $v = 0.542$. These parameter values were assumed to hold for all members of the series. The consideration of intensities of reflection of Sc_2O_3 then was found to indicate the $48\,O$ to be in two groups of 24 in the general position of T^5, with parameters $x_1 \sim \frac{1}{8}$, $y_1 \sim \frac{1}{8}$, $z_1 \sim \frac{3}{8}$ and $x_2 \sim \frac{1}{8}$, $y_2 \sim \frac{3}{8}$, $z_2 \sim \frac{3}{8}$. The same structure was also assigned bixbyite, with $16\,(Mn, Fe)_2O_3$ in a unit 9.35 ± 0.02 Å on edge.

On beginning the investigation of the tetragonal pseudo-cubic mineral braunite, $3\,Mn_2O_3 . MnSiO_3$, we found the unit of structure to be closely related to that of bixbyite, and, indeed, to have dimensions nearly the same as those for two superimposed bixbyite cubes. This led us to

1) V. M. Goldschmidt, »Geochem. Vert.-Ges. d. El.« IV, V, Videnskapsselsk. Skr., **5**, 7, Oslo. 1925. 2) W. Zachariasen, Z. Krist. **67**, 455. 1928; »Untersuchungen über die Kristallstruktur von Sesquioxyden und Verbindungen ABO_3«, Videnskapsselsk. Skr. **4**, Oslo. 1928.

make a study of Zachariasen's structure, leading to the observation that not only are the interatomic distances reported abnormally small, but also the structure does not fall in line with the set of principles found to hold for coordinated structures in general[1]). It was further noted that Zachariasen's atomic arrangement, with the symmetry of space group T^5, approximates very closely an arrangement with the symmetry of T_h^7 (of which T^5 is a sub-group), and it is difficult to find a physical explanation of this distortion from a more symmetrical structure. This led to the reinvestigation of this mineral and the determination of a new and satisfactory structure for the *C*-modification of the sesquioxides.

2. The Unit of Structure and Space-group Symmetry of Bixbyite.

Bixbyite, found only in Utah, about 35 miles southwest of Simpson, is described by Penfield and Foote[2]) as forming shiny black cubic crystals with a trace of octahedral cleavage. The composition assigned it by them was $Fe^{++}Mn^{+4}O_3$, with a little isomorphous replacement of Fe^{++} by Mg^{++} and Mn^{++} and of Mn^{+4} by Ti^{+4}. It was shown by Zachariasen that the X-ray data exclude this formulation, and indicate instead that the mineral is a solid solution of Mn_2O_3 and Fe_2O_3. We shall reach a similar conclusion.

Table I.

Spectral Data from (100) of Bixbyite
(with rock salt comparison).

hkl	Line	*d/n*	Estimated Intensity	$S^2/10{,}000$
200	$MoK\alpha_1$	$\frac{1}{2} \times 9.40$ Å	0.05	0.26
400	α_1	$\frac{1}{4} \times 9.38$	7	21.16
400	α_2	$\frac{1}{4} \times 9.37$		
600	α_1	$\frac{1}{6} \times 9.38$	0.2	0.64
600	α_2	$\frac{1}{6} \times 9.36$		
800	α_1	$\frac{1}{8} \times 9.36$	5	20.0
800	α_2	$\frac{1}{8} \times 9.34$		
10.0.0	α_1	$\frac{1}{10} \times 9.38$	0.1	0.23
10.0.0	α_2	$\frac{1}{10} \times 9.34$		
12.0.0	α_1	$\frac{1}{12} \times 9.36$	0.4	1.80
14.0.0	α_1	$\frac{1}{14} \times 9.37$	0.3	0.71
16.0.0	—	—	0.1	0.71

Average: $a = 9.365 \pm 0.020$ Å.

1) Linus Pauling, J. Am. chem. Soc, **51**, 1010. 1929.

2) S. L. Penfield and H. W. Foote, Z. Krist. **28**, 592. 1897.

Data from oscillation photographs of bixbyite show a to be a multiple of 4.68 Å (Table I). The Polanyi layer-line relation applied to photographs with [100] as rotation axis showed that this multiple must be 2, giving a unit with

$$a = 9.365 \pm 0.020 \text{ Å}.$$

This unit sufficed to account for the occurrence of all spots observed on several Laue photographs taken with a tube operated at a peak voltage of 54 kv. (the incident beam making small angles with [100] or [110]), and may be accepted as the true unit.

Table II.

Laue Data for Bixbyite.

Incident beam nearly normal to (100).

$\{hkl\}$	d_{hkl} Å	Estimated Intensity. $n\lambda =$				S Calculated	$S^2/10{,}000$
		0.25—0.29 Å	0.30—0.34 Å	0.35—0.39 Å	0.40—0.45 Å		
611	1.51				10.0	209	4.37
451	1.44				10.0	172	2.96
415					10.0	157	2.46
631	1.38			7.0	7.0	218	4.75
613				7.0	10.0	— 233	5.43
271	1.27		0.4	1.0		119	1.42
217			2.5	3.0		— 154	2.37
651	1.18	0.1	0.4			139	1.93
615		0.2	0.4			142	2.02
417	1.15	0.1	0.1			— 84	0.71
471			0.8			107	1.14
811	1.15	1.0	1.6			180	3.24
275	1.06				0.0	18	0.03
257					0.1	25	0.06
219	1.01				0.0	11	0.01
291					0.2	30	0.09
293	0.96			0.1	0.1	43	0.18
239				0.1	0.2	43	0.18
277	.93			0.3	0.4	— 103	1.06
837	.85				0.6	— 102	1.04
873					0.6	— 107	1.14
10.5.3	.84			0.1	0.05	— 93	0.86
10.3.5					0.1	93	0.86
4.11.3	.77			0.1	0.1	— 63	0.40
4.3.11				0.1	0.1	— 68	0.46

The value 4.945 for the density of bixbyite reported by Penfield and Foote leads to 16 $(Mn, Fe)_2O_3$ in the unit.

It was observed that the only planes giving odd-order reflections (see Table II) were those with $h+k+l$ even, indicating strongly that the structure is based on the body-centered cubic lattice I''_c. Moreover, a Laue photograph taken with the incident beam normal to (100) showed only two symmetry planes and a two-fold axis, requiring that the point-group symmetry of the crystal be that of T or T_h. The only space groups compatible with these conditions are T^3, T^5, T_h^5, and T_h^7. Of these T_h^7 requires that planes $(0kl)$ with k and l odd give no odd-order reflections, while T^3, T^5, and T_h^5 allow such reflections to occur. On our photographs no such reflections were found, although a number of planes of this type were in positions favorable to reflection (Table III). This makes it highly probable that T_h^7 is the correct space group, for it would be very difficult to account for the absence of these reflections with an atomic arrangement derived from T^3, T^5, or T_h^5 which at the same time did not come indistinguishably close to an arrangement derivable from T_h^7. In view of these considerations we have assumed T_h^7 to be the correct space group.

Table III.

Data for Prism Forms from Bixbyite.

A. Forms not reflecting on Laue photographs:

$\{hkl\}$	$n\lambda$	
{071}	0.35,	0.39 Å
{701}	0.34,	0.40
{11.0.3}	0.40,	0.45
{0.11.3}	0.41,	0.44
{13.0.3}	0.30,	0.33
{0.13.3}	0.31,	0.32

B. Forms not reflecting on oscillation photographs:

{031}, {013}, {033}, {051}, {015}, {053}, {035}, {055},
{071}, {017}, {073}, {037}, {075}, {057}, {091}, {019},
{093}, {039}, {095}, {059}.

This choice of space group is further substantiated by Zachariasen's data for the other substances as well as bixbyite. His reproduced Laue photographs of Tl_2O_3 and of bixbyite show no spots due to {071}, {017}, {091}, {019}, {0.11.1} or {0.1.11}, although planes of these forms were in positions favorable to reflection, while the powder data show that {031}, {013}, {073}, and {037} gave no reflections for any of the sesquioxides studied. Zachariasen's rejection of T_h^7 arose from his

assumption that the oxygen contribution to the intensities was negligible, and his consequent inability to account for the observed inequalities in intensity of pairs of forms such as {271} and {217} with the metal atoms in positions provided by T_h^7. But actually the oxygen contribution is by no means negligible. For example, the structure which we find gives for the metal contributions to the structure factor for {271} and {217} the values + 66.2 and — 66.2, which are changed by the oxygen contribution to + 119.6 and — 154.2, respectively. For Tl_2O_3 the effect of the oxygen would be only about one-fourth as great, which is, however, still sufficient to account for the observed inequalities[1]).

3. The Arrangement of the Metal Atoms.

The equivalent positions provided by T_h^7 are:

8*i*: $0\,0\,0$; $\frac{1}{2}\,\frac{1}{2}\,0$; $\frac{1}{2}\,0\,\frac{1}{2}$; $0\,\frac{1}{2}\,\frac{1}{2}$;
$\frac{1}{2}\,\frac{1}{2}\,\frac{1}{2}$; $0\,0\,\frac{1}{2}$; $0\,\frac{1}{2}\,0$; $\frac{1}{2}\,0\,0$.

8*e*: $\frac{1}{4}\,\frac{1}{4}\,\frac{1}{4}$; $\frac{1}{4}\,\frac{3}{4}\,\frac{3}{4}$; $\frac{3}{4}\,\frac{1}{4}\,\frac{3}{4}$; $\frac{3}{4}\,\frac{3}{4}\,\frac{1}{4}$;
$\frac{3}{4}\,\frac{3}{4}\,\frac{3}{4}$; $\frac{3}{4}\,\frac{1}{4}\,\frac{1}{4}$; $\frac{1}{4}\,\frac{3}{4}\,\frac{1}{4}$; $\frac{1}{4}\,\frac{1}{4}\,\frac{3}{4}$.

16*e*: $u\,u\,u$; $u, \bar{u}, \frac{1}{2}-u$; $\frac{1}{2}-u, u, \bar{u}$; $\bar{u}, \frac{1}{2}-u, u$;
$\bar{u}\,\bar{u}\,\bar{u}$; $\bar{u}, u, u+\frac{1}{2}$; $u+\frac{1}{2}, \bar{u}, u$; $u, u+\frac{1}{2}, \bar{u}$;
$u+\frac{1}{2}, u+\frac{1}{2}, u+\frac{1}{2}$; $u+\frac{1}{2}, \frac{1}{2}-u, \bar{u}$; $\bar{u}, u+\frac{1}{2}, \frac{1}{2}-u$; $\frac{1}{2}-u, \bar{u}, u+\frac{1}{2}$;
$\frac{1}{2}-u, \frac{1}{2}-u, \frac{1}{2}-u$; $\frac{1}{2}-u, u+\frac{1}{2}, u$; $u, \frac{1}{2}-u, u+\frac{1}{2}$; $u+\frac{1}{2}, u, \frac{1}{2}-u$.

24*e*: $u\,0\,\frac{1}{4}$; $\bar{u}\,\frac{1}{2}\,\frac{1}{4}$; $\frac{1}{2}-u, 0, \frac{3}{4}$; $u+\frac{1}{2}, \frac{1}{2}, \frac{3}{4}$;
$\frac{1}{4}\,u\,0$; $\frac{1}{2}\,\bar{u}\,\frac{1}{2}$; $\frac{3}{4}, \frac{1}{2}-u, 0$; $\frac{3}{4}, u+\frac{1}{2}, \frac{1}{2}$;
$0\,\frac{1}{4}\,u$; $\frac{1}{2}\,\frac{1}{4}\,\bar{u}$; $0, \frac{3}{4}, \frac{1}{2}-u$; $\frac{1}{2}, \frac{3}{4}, u+\frac{1}{2}$;
$\bar{u}\,0\,\frac{3}{4}$; $u\,\frac{1}{2}\,\frac{3}{4}$; $u+\frac{1}{2}, 0, \frac{1}{4}$; $\frac{1}{2}-u, \frac{1}{2}, \frac{1}{4}$;
$\frac{3}{4}\,\bar{u}\,0$; $\frac{3}{4}\,u\,\frac{1}{2}$; $\frac{1}{4}, u+\frac{1}{2}, 0$; $\frac{1}{4}, \frac{1}{2}-u, \frac{1}{2}$;
$0\,\frac{3}{4}\,\bar{u}$; $\frac{1}{2}\,\frac{3}{4}\,u$; $0, \frac{1}{4}, u+\frac{1}{2}$; $\frac{1}{2}, \frac{1}{4}, \frac{1}{2}-u$.

48: $x\,y\,z$; $x, \bar{y}, \frac{1}{2}-z$; $\frac{1}{2}-x, y, \bar{z}$; $\bar{x}, \frac{1}{2}-y, z$;
$z\,x\,y$; $\frac{1}{2}-z, x, \bar{y}$; $\bar{z}, \frac{1}{2}-x, y$; $z, \bar{x}, \frac{1}{2}-y$;
$y\,z\,x$; $\bar{y}, \frac{1}{2}-z, x$; $y, \bar{z}, \frac{1}{2}-x$; $\frac{1}{2}-y, z, \bar{x}$;
$\bar{x}\,\bar{y}\,\bar{z}$; $\bar{x}, y, z+\frac{1}{2}$; $x+\frac{1}{2}, \bar{y}, z$; $x, y+\frac{1}{2}, \bar{z}$;
$\bar{z}\,\bar{x}\,\bar{y}$; $z+\frac{1}{2}, \bar{x}, y$; $z, x+\frac{1}{2}, \bar{y}$; $z, x, y+\frac{1}{2}$;
$\bar{y}\,\bar{z}\,\bar{x}$; $y, z+\frac{1}{2}, \bar{x}$; $\bar{y}, z, x+\frac{1}{2}$; $y+\frac{1}{2}, \bar{z}, x$;
$x+\frac{1}{2}, y+\frac{1}{2}, z+\frac{1}{2}$; $x+\frac{1}{2}, \frac{1}{2}-y, z$; $\bar{x}, y+\frac{1}{2}, \frac{1}{2}-z$; $\frac{1}{2}-x, \bar{y}, z+\frac{1}{2}$;
$z+\frac{1}{2}, x+\frac{1}{2}, y+\frac{1}{2}$; $z, x+\frac{1}{2}, \frac{1}{2}-y$; $\frac{1}{2}-z, \bar{x}, y+\frac{1}{2}$; $z+\frac{1}{2}, \frac{1}{2}-x, \bar{y}$;
$y+\frac{1}{2}, z+\frac{1}{2}, x+\frac{1}{2}$; $\frac{1}{2}-y, z, x+\frac{1}{2}$; $y+\frac{1}{2}, \frac{1}{2}-z, \bar{x}$; $\bar{y}, z+\frac{1}{2}, \frac{1}{2}-x$;
$\frac{1}{2}-x, \frac{1}{2}-y, \frac{1}{2}-z$; $\frac{1}{2}-x, y+\frac{1}{2}, z$; $x, \frac{1}{2}-y, z+\frac{1}{2}$; $x+\frac{1}{2}, y, \frac{1}{2}-z$;
$\frac{1}{2}-z, \frac{1}{2}-x, \frac{1}{2}-y$; $z, \frac{1}{2}-x, y+\frac{1}{2}$; $z+\frac{1}{2}, x, \frac{1}{2}-y$; $\frac{1}{2}-z, x+\frac{1}{2}, y$;
$\frac{1}{2}-y, \frac{1}{2}-z, \frac{1}{2}-x$; $y+\frac{1}{2}, z, \frac{1}{2}-x$; $\frac{1}{2}-y, z+\frac{1}{2}, x$; $y, \frac{1}{2}-z, x+\frac{1}{2}$.

1) Dr. Zachariasen has kindly informed us that he now agrees with our choice of the space group T_h^7.

Of these, all but the general position may be occupied by the metal atoms. The 32 metal atoms may have any one of the following arrangements:

A: Formula, $FeMnO_3$:

1a. 16 *Fe* in 16*e*, 16 *Mn* in 16*e*.
2a. 16 *Fe* in 16*e*, 8 *Mn* in 8*i*, 8 *Mn* in 8*e*.
2b. 16 *Mn* in 16*e*, 8 *Fe* in 8*i*, 8 *Fe* in 8*e*.

B: Formula, $(Mn, Fe)_2O_3$:

1b. 16 (*Mn*, *Fe*) in 16*e*, 16 (*Mn*, *Fe*) in 16*e*.
2c. 16 (*Mn*, *Fe*) in 16*e*, 8 (*Mn*, *Fe*) in 8*i*, 8 (*Mn*, *Fe*) in 8*e*.
3. 24 (*Mn*, *Fe*) in 24*e*, 8 (*Mn*, *Fe*) in 8*i*, or
24 (*Mn*, *Fe*) in 24*e*, 8 (*Mn*, *Fe*) in 8*e*.

The reflecting powers of *Mn* and *Fe* are nearly the same, and may be taken equal without serious error. This reduces the number of distinct structures to three; namely, 1*ab*, 2*abc*, and 3, of which 1*ab* depends on two parameters and the others on one. It is possible to decide among them in the following way. Let us assume that the contribution of oxygen atoms to the intensity of reflection in various orders from (100) is small compared with the maximum possible contribution of the metal atoms; that is, with $32\bar{M}$. The metal atom structure factor for structure 1 for $(h00)$ is

$$S_{h00} = 16\bar{M}\,(\cos 2\pi h u_1 + \cos 2\pi h u_2).$$

Now (200) gave a very weak reflection, so that S_{200} must be small. This is true only for $u_1 + u_2 \simeq \frac{1}{4}$, for which

$$S_{h00} \simeq 0 \text{ for } h = 2, 6, 10,$$
$$S_{h00} \simeq 32\bar{M} \cos 2\pi h u_1 \text{ for } h = 4, 8, 12.$$

Now the gradual decline in intensity for $h = 4, 8, 12$ (Table I) requires that $u_1 = \frac{1}{8}$, and hence $u_2 = \frac{1}{8}$. This puts the two sets of metal atoms in the same place, and is hence ruled out. It may also be mentioned that structure 1 would place eight metal atoms on a cube diagonal, giving a maximum metal-metal distance of 2.03 Å, which is considerably smaller than metal-metal distances observed in other crystals. Structure 2, dependent on one parameter u, has structure factors

$$S_{h00} = 16\bar{M} \cos 2\pi h u \text{ for } h = 2, 6, \ldots,$$
$$S_{h00} = 16\bar{M}\,(1 + \cos 2\pi h u) \text{ for } h = 4, 8, \ldots.$$

All values of the parameter u are eliminated by the comparisons $600 > 200$, $400 > 200$, and $10.0.0 > 200$.

There accordingly remains only structure 3. We may take $8(Mn, Fe)$ in $8e$ rather than $8i$, which leads to the same arrangements. The structure factor for various orders from (100) is then

$$S_{h00} = 8\bar{M}\,(\cos 2\pi h u - 1) \text{ for } h = 2,\ 6,\ 10,\ \text{etc.}$$
$$S_{h00} = 8\bar{M}\,(\cos 2\pi h u + 3) \text{ for } h = 4,\ 8,\ 12,\ \text{etc.}$$

All distinct structures are included in the parameter range $-0.25 \leqslant u \leqslant 0.25$, and, moreover, positive and negative values of u give the same intensity of reflection from $(h\,0\,0)$. Hence we need consider only $0 \leqslant |u| \leqslant 0.25$. In Figure 1 are shown values of $|S|$ calculated over

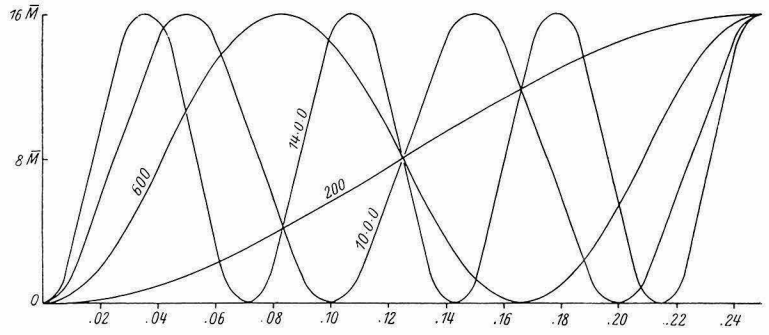

Fig. 1. Structure factor curves over the range $0 \leqslant |u| \leqslant 0.25$ with $\bar{M}$ constant.

this range with a constant value for $\bar{M}$. It is seen that the observed intensity inequality $600 > 200$ rules out the region $0.125 \leqslant |u| \leqslant 0.25$, and $10.0.0 > 200$ and $14.0.0 > 200$ further limit $|u|$ to between 0.00 and 0.06. The value of $|u|$ can be more closely determined by the use of atomic amplitude curves. The intensity of the diffracted beam can be taken as

$$I = K \cdot A_{hkl}^2, \tag{1}$$

with

$$A_{hkl} = \sum_i A_i\, e^{2\pi i\,(hx_i + ky_i + lz_i)}. \tag{2}$$

In this expression A_i, the atomic amplitude function, is given by

$$A_i = \left\{\frac{1 + \cos^2 2\theta}{2 \sin 2\theta}\right\}^{\frac{1}{2}} \cdot F_i, \tag{3}$$

in which F_i is the atomic F-function. Values of A_{Fe} and A_O calculated for MoK_α radiation and for an average wave-length of 0.40 Å effective on Laue photographs from Bragg and West's F-curves[1]) are given in

1) W. L. Bragg and J. West, Z. Krist. **69**, 118. 1928.

Table IV. Figure 2 shows values of A_{h00} for $h = 2, 4 \ldots 16$ over the range of values 0 to 0.06 for $|u|$. It is seen that the value $|u| = 0.030 \pm 0.005$ is indicated by the observed intensities of Table I.

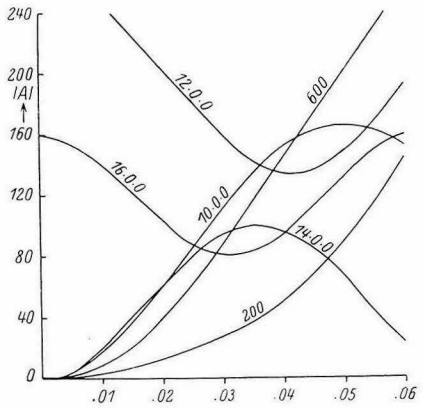

Fig. 2. A-curves over the range $0 \ll |u| \ll 0.06$.

Table IV.

Atomic A-values for Iron and Oxygen.

d_{hkl}	$\lambda = 0.40$ Å		$\lambda = 0.709$ Å	
	A_O	A_{Fe}	A_O	A_{Fe}
5.00 Å	28.0	79.0	21.2	59.8
2.50	14.5	45.0	10.4	33.6
1.67	7.5	30.1	5.8	21.7
1.25	4.4	21.8	3.5	15.6
1.00	2.7	16.8	2.1	11.6
0.83	1.5	12.5	1.2	9.0
0.72	0.9	10.3	0.6	7.3
0.63	0.6	8.4	0.4	5.9
0.55	0.4	6.6	0.2	4.6
0.50	0.3	5.2	0.1	4.0
0.45	—	4.5	—	3.6
0.42	—	3.7	—	3.4
0.39	—	3.1	—	3.2

Now there are two physically distinct arrangements of the metal atoms corresponding to $|u| = 0.030$, the first with $u = 0.030$, and the second with $u = -0.030$; and it is not possible to distinguish between them with the aid of the intensities of reflection of X-rays which they give. Let us consider the positions $24e$. The structure factor for $24e$ is:

$$S_{hkl} = 8\overline{M}[\cos 2\pi(hu + l/4) + \cos 2\pi(ku + h/4) + \cos 2\pi(lu + k/4)]$$
for h, k, l all even;
$$= 8\overline{M}\cos 2\pi(hu + l/4) \text{ for } h \text{ even, } k \text{ odd, } l \text{ odd;}$$
$$= 8\overline{M}\cos 2\pi(ku + h/4) \text{ for } h \text{ odd, } k \text{ even, } l \text{ odd;}$$
$$= 8\overline{M}\cos 2\pi(lu + k/4) \text{ for } h \text{ odd, } k \text{ odd, } l \text{ even.}$$
$$= 0 \text{ otherwise.}$$

It is seen that the value of the structure factor is the same for a given positive as for the same negative value of u, except for a difference in sign in some cases. But the positive and the negative parameter values correspond to structures which are not identical, but are distinctly different, as can be seen when the attempt to bring them into coincidence is made. This is a case where two distinct structures give the same intensity of X-ray reflections from all planes, so that they could not be distinguished from one another by X-ray methods. The presence of atoms in $8e$ or $8i$ does not change this result. In the case of bixbyite a knowledge of the positions of the oxygen atoms would enable the decision between these alternatives to be made, but the rigorous evaluation of the three oxygen parameters from the X-ray data cannot be carried out.

Zachariasen's arrangement of the metal atoms approximates the first of our two (that with the positive parameter value), and would be identical with it if his parameters were taken to be 0.030 and 0.530 rather than 0.021 and 0.542.

4. The Prediction and Verification of the Atomic Arrangement.

Recognizing the impracticability of determining the positions of the oxygen atoms from X-ray data, we have predicted a set of values for the oxygen parameters with the use of assumed minimum interatomic distances which is found to account satisfactorily for the observed intensities of a large number of reflections and which also leads to a structure which is physically reasonable.

The $Fe—O$ distances in hematite are 1.99 and 2.06 Å. The $(Mn, Fe)—O$ distances in bixbyite are expected to be the same in case that (Mn, Fe) has the coordination number 6, and slightly smaller, perhaps 1.90 Å, for coordination number 4. The radius of $O^=$ is 1.40 Å, and the average $O—O$ distance in oxide crystals has about twice this value. When coordinated polyhedra share edges the $O—O$ distance is decreased to a minimum value of 2.50 Å, shown by shared edges in rutile, anatase, brookite, corundum, hydrargillite, mica, chlorite, and other crystals. Our experience with complex ionic crystals leads us to believe that we may

safely assume that the $(Mn, Fe)—O$ and the $O—O$ distances in bixbyite will not fall below 1.80 Å and 2.40 Å respectively.

On attempting to build up a structure on the basis of the first arrangement of the metal atoms, with $u = 0.030$, we found that there is no way in which the oxygen atoms can be introduced without causing interatomic distances smaller than the assumed minimum ones. This arrangement (which approximates Zachariasen's) is accordingly eliminated.

The second arrangement of the metal atoms, with $u = -0.030$, is such that satisfactory interatomic distances are obtained only when the oxygen atoms are in the general position with $x \simeq \frac{3}{8}$, $y \simeq \frac{1}{8}$, and $z \simeq \frac{3}{8}$. Each oxygen atom is then at about 2 Å from four metal atoms; if it be assumed that these four metal-oxygen distances are equal, the parameters are found to have the values

$$x = 0.385, \qquad y = 0.145, \qquad z = 0.380.$$

With this structure each metal atom is surrounded by six oxygen atoms at a distance of 2.01 Å, and the minimum $O—O$ distance is 2.50 Å. These dimensions are entirely reasonable.

It is probable that the various metal-oxygen distances are not exactly equal, but show variations of possibly $\pm$ 0.05 Å. The predicted parameter values may correspondingly be assumed to be accurate to only about $\pm$ 0.005.

Table V. Data from an Oscillation Photograph of Bixbyite[1].

$\{h\,0\,l\}$	Estimated Intensity	$S^2/10{,}000$
202	0.00	0.01
402	0.01	0.28
404	10	67.00
602	0.2	0.68
604	0.6	1.69
802	0.2	0.74
804	2	3.34
806	0.05	0.19

The predicted structure has been verified by the comparison of the observed intensities of reflection for a large number of planes and those calculated with the use of Equation 1. Data for such comparisons for planes $(h\,0\,0)$ and $(h\,0\,l)$ reflecting on oscillation photographs are given in Tables I and V, and for other planes giving Laue reflections in

1) These reflections are from the first, second, and third layer lines of the same photograph as that from which the data of Table I were obtained, so that intercomparisons between Tables I and V may be made.

Table II. It is seen that the agreement between calculated and observed intensities is almost complete; the existent discrepancies are generally explicable as resulting from small errors in the parameter values (within the limits $\pm$ 0.005) or from errors in the assumed F-curves, for which an accuracy greater than $\pm$ 20% is not claimed.

5. Description of the Structure.

The structure found by the methods just described agrees well with the general principles underlying complex ionic crystals. The arrangement of the metal ions is shown in Fig. 3. These ions are nearly in cubic close-packing, so that the structure gives nearly the maximum dispersion of cations with given molal volume. Each cation is surrounded by six oxygen ions at a distance of 2.01 Å, at the corners of a highly distorted octahedron. These octahedra are of two types, corresponding to the two positions $8e$ and $24e$. Each $8e$ octahedron (with point-group symmetry C_{3i}) shares six edges with adjoining $24e$ octahedra, and each $24e$ octahedron shares six edges also, two with $8e$ and four with other $24e$ octahedra. Every shared edge is 2.50—2.52 Å long, in striking agreement with the minimum dimensions found in other crystals for shared edges and the theoretical values obtained for rutile and anatase[1]). These shared edges are arranged differently for $8e$ and $24e$; the distortion accompanying their shortening leads to octahedra of the shapes shown in Fig. 4 and 5. Various interatomic distances are given in Table VI.

Table VI.

Interatomic Distances in Bixbyite.

$(Fe,Mn)-O_A=2.01$ Å	$(Fe,Mn)-O_K=2.01$ Å	$O_A-O_F=2.52$ Å	$O_H-O_E=3.29$Å
$(Fe,Mn)-O_B=2.01$	$(Fe,Mn)-O_L=2.01$	$O_B-O_E=2.52$	$O_L-O_G=3.29$
$(Fe,Mn)-O_C=2.01$	$O_A-O_B=3.13$	$O_B-O_F=2.52$	$O_H-O_I=2.50$
$(Fe,Mn)-O_D=2.01$	$O_B-O_C=3.13$	$O_C-O_D=2.52$	$O_K-O_L=2.50$
$(Fe,Mn)-O_E=2.01$	$O_D-O_E=3.13$	$O_C-O_E=2.52$	$O_H-O_K=2.51$
$(Fe,Mn)-O_F=2.01$	$O_D-O_F=3.13$	$O_K-O_I=3.38$	$O_I-O_L=2.51$
$(Fe,Mn)-O_G=2.01$	$O_E-O_F=3.13$	$O_G-O_E=2.92$	$O_G-O_K=2.50$
$(Fe,Mn)-O_H=2.01$	$O_A-O_C=3.13$	$O_H-O_G=3.12$	$O_E-O_I=2.50$
$(Fe,Mn)-O_I=2.01$	$O_A-O_D=2.52$	$O_L-O_E=3.12$	

Each oxygen ion is common to four octahedra, and has $\sum_i' s_i = 2$, in accordance with the electrostatic valence rule.

The structure can be instructively compared with that of fluorite, CaF_2. In fluorite the calcium ions are arranged at face-centered lattice points, and each is surrounded by eight fluorine ions at cube corners.

1) Linus Pauling, Z. Krist. **67**, 377. 1928.

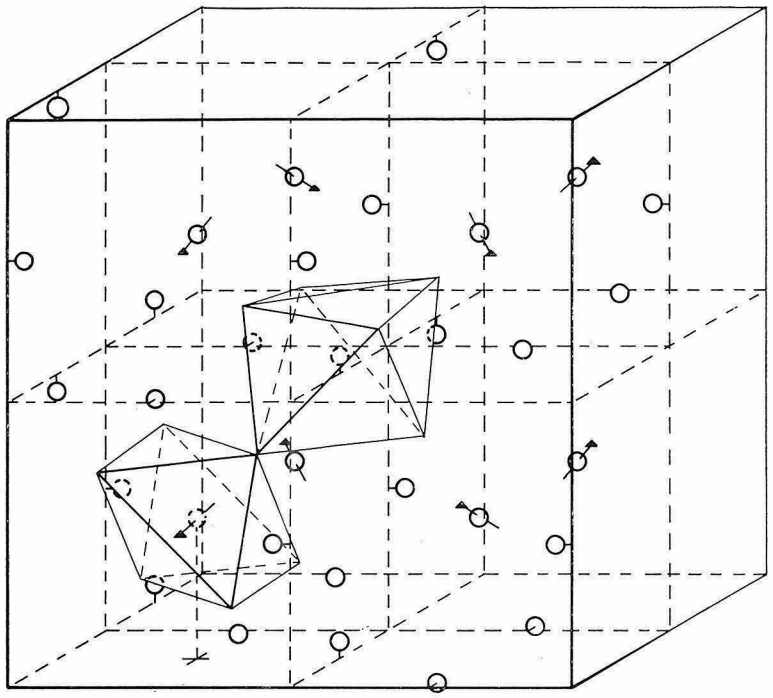

Fig. 3. The structure of bixbyite. The metal ions are shown, together with one of each kind of distorted octahedron.

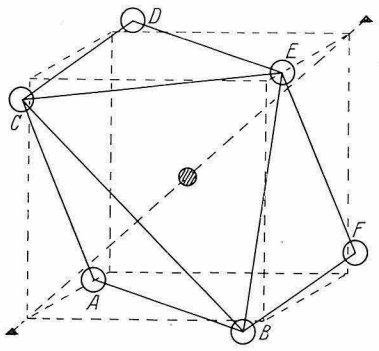

Fig. 4. The 8*e* octahedron, showing its relation to a cube.

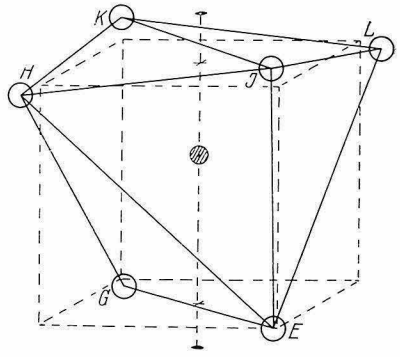

Fig. 5. The 24*e* octahedron, showing its relation to a cube.

If one-fourth of the fluorine ions are removed and the others are replaced by oxygen ions, calcium being replaced by (*Mn*, *Fe*), a structure is obtained which approximates that of bixbyite, which differs from it only in small displacements of the ions. This similarity is shown by the fact that the highly distorted octahedra have corners which are nearly at six of the eight corners of a cube, the six being chosen differently for the 8*e* and the 24*e* octahedra, as is seen from Fig. 4 and 5. This analogy was, indeed, pointed out by Zachariasen for his incorrect structure. As a matter of fact the "ideal" structure, with $u = 0$ and

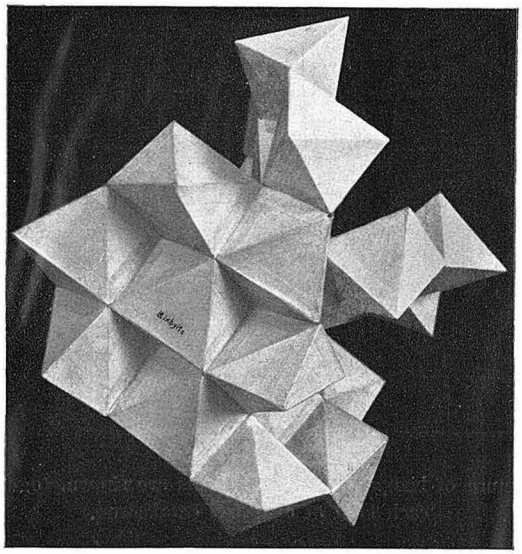

Fig. 6. A photograph of a model representing one half of the unit cube. The arrangement of the six 24*e* octahedra sharing edges with an 8*e* octahedron is clearly shown.

$x = \frac{3}{8}$, $y = \frac{1}{8}$, $z = \frac{3}{8}$, corresponding to Zachariasen's original atomic arrangement also corresponds to ours. Zachariasen very instructively pointed out that this ideal structure lies midway between the fluorite and the sphalerite arrangements, being obtained either by removing certain anions from fluorite, or by adding anions to sphalerite, the positions of the other ions remaining unchanged in either case. With the ideal structure the coordinated polyhedra are cubes with two truncated corners; for 8*e* these corners are at the ends of a body diagonal, for 24*e* at the ends of a face diagonal. The actual structure is distorted from the ideal one, which leads to too small interionic distances, in such a way as to give a constant metal-oxygen distance and a minimum oxygen-oxygen distance (for shared edges) of 2.50 Å. In Zachariasen's arrangement the distortion was in the opposite direction.

Table VII. Interatomic Distances in Sesquioxides.

Substance	a	$M-O$
$(Fe, Mn)_2O_3$	9.365 Å	2.01 Å
Mn_2O_3	9.41	2.02
Sc_2O_3	9.79	2.10
Y_2O_3	10.60	2.27
In_2O_3	10.12	2.17
Tl_2O_3	10.57	2.26
Sm_2O_3	10.85	2.33
Eu_2O_3	10.84	2.33
Gd_2O_3	10.79	2.32
Tb_2O_3	10.70	2.30
Dy_2O_3	10.63	2.28
Ho_2O_3	10.58	2.27
Er_2O_3	10.54	2.26
Tm_2O_3	10.52	2.26
Yb_2O_3	10.39	2.23
Lu_2O_3	10.37	2.22

As mentioned by Zachariasen, Goldschmidt[1]) found that the range of radius-ratio values leading to stability of the C-modification is about $0.60 < \frac{R_{M^{+3}}}{R_{O^=}} < 0.88$, which is high[2]) for a structure in which the coordination number is 6. The explanation of this is obvious; the coordinated octahedra are deformed so that the anions are nearly at six cube corners, and the radius ratio will accordingly tend to the range of values giving the coordination number 8.

A photograph of a model representing the structure is shown in Fig. 6.

Zachariasen's investigation makes it highly probable that the sesquioxides forming crystals of the C-modification have the same structure as that which we have found for bixbyite, and the similarity in intensities on powder photographs of the different substances which he reports indicates that the parameter values do not change very much throughout the series. Thus in all these crystals the cations are attributed the coordination number 6. Values of interionic distances calculated from Zachariasen's values of a with the bixbyite parameters are given in Table VII. It is probable, however, that the oxygen parameters do change as a increases in such a way as to keep shared edges short, for with the bixbyite parameters the shared edges increase from 2.50 Å to about 2.90 Å in Sm_2O_3 and Eu_2O_3. As a consequence the metal-oxygen dis-

1) V. M. Goldschmidt, »Geochem. Vert.-Ges. d. El.«, VII, p. 76.

2) Linus Pauling, J. Am. chem. Soc. **51**, 1010. 1929.

tances in Table VII are probably a little larger than the true ones, the maximum error being 0.10 Å. It is worthy of mention that the C-structure and the corundum structure correspond to nearly the same interionic distances (1.99—2.06 A in hematite as compared with 2.01 Å in bixbyite), as is to be expected from the equality in coordination number of the cation.

Summary.

With the use of data from oscillation and Laue photographs it is shown that the unit of structure of bixbyite has $a = 9.365$ Å and contains $16(Mn, Fe)_2O_3$. The lattice is the body-centered cubic one, I''_c, and the space group is T_h^7. Two possible arrangements alone of the metal atoms are found to be compatible with the X-ray data (oxygen atoms being neglected), the first with $8(Mn, Fe)$ in $8e$, $24(Mn, Fe)$ in $24e$ with $u = 0.030$, and the second the same except with $u = -0.030$. It is pointed out that these two physically distinct arrangements give the same intensities of reflection of X-rays from all planes, so that an unambiguous structure determination for a crystal containing only atoms in $24e$ (or $24e$, $8e$, $8i$) could not be made with X-ray methods alone, despite the dependence on only one parameter.

The assumption that the $(Mn, Fe)—O$ and $O—O$ distances can not fall below 1.80 Å and 2.40 Å, respectively, eliminates the first metal atom arrangement, for there are no positions for oxygen satisfying it. With the second arrangement of metal atoms this assumption requires $48\ O$ to be in the general position of T_h^7, with $x \simeq \frac{3}{8}$, $y \simeq \frac{1}{8}$, $z \simeq \frac{3}{8}$. Each oxygen ion is then nearly equidistant from four cations. Making the four $(Mn, Fe)—O$ distances equal, values of the parameters are predicted which lead to good agreement between observed and calculated intensities of reflection from a large number of planes. The structure found for bixbyite has

$8(Mn, Fe)$ in $8e$

$24(Mn, Fe)$ in $24e$ with $u = -0.030 \pm 0.005$

$48\ O$ in x, y, z, etc. with $x = 0.385 \pm 0.005$,

$y = 0.145 \pm 0.005$,

$z = 0.380 \pm 0.005$.

A description of the structure with values of interatomic distances for bixbyite and for Sc_2O_3, Mn_2O_3, Y_2O_3, In_2O_3, Tl_2O_3, Sm_2O_3, Eu_2O_3, Gd_2O_3, Tb_2O_3, Dy_2O_3, Ho_2O_3, Er_2O_3, Tm_2O_3, Yb_2O_3, and Lu_2O_3, which are shown to have the same structure by Zachariasen's investigation, is given in Section 5.

Received July 5th, 1930.

Printed in Germany.